DOCTORAL DISSERTATION

Development of a Genetically Encoded Monomeric Green Photosensitizer for Light-inducible Protein Inactivation and Cell Ablation

Yemima Dani Riani

July 2018

Graduate School of Engineering

Osaka University

GENERAL INTRODUCTION

In order to get better understanding of a biological system, one of many questions often addressed in research is: “What is the function of particular of protein/cell function within cell/organism?” A well-established method to answer that question is by analyzing the loss-of-function phenotype. Currently available methods, such as gene knockout, knockdown, toxin- or laser-mediated cell ablation, have drawbacks to achieve high precision of target inactivation/ablation in spatiotemporal controlled manner. Photosensitizer, which is chromophore that generates ROS (Reactive Oxygen Species) upon light irradiation, had shown its great performance to perform such task.

Chapter 1 describes all properties of currently available photosensitizers and introduces genetically encoded photosensitizer that has excellent specificity to targeting molecules. Since colour variants of genetically encoded photosensitizer are activated by different excitation wavelengths, utilizing those would enable several different protein/cells to be inactivated in a defined time and area in intact systems. In order to achieve this, a green colour variant of currently available photosensitizing protein, SuperNova Red, is developed in this study and named SuperNova Green. *In vitro* characterization has shown that SuperNova Green emits green emission when excited with blue light. SuperNova Green also maintains SuperNova Red monomeric property and shows its superiority over dimeric photosensitizing proteins when fused with target protein or localization signal.

Chapter 2 describes characterization of SuperNova Green ROS production. As known that different type of ROS would have different target, specificity and diffusion range, it is important to know that which type of ROS does SuperNova Green produce. As

characterization result, SuperNova Green produces superoxide and its derivatives (hydrogen peroxide and hydroxyl radical) that are common type of ROS generated naturally in cells, for example, through oxidative phosphorylation in mitochondria or other enzymatic reactions.

Chapter 3 shows the usefulness of SuperNova Green to inactivate protein and promote cell ablation. As proof of concept of multiple protein inactivation and cell ablation, SuperNova Green in combination with SuperNova Red could selectively inactivate Pleckstrin Homology domain of Phospholipase C-δ1 and ablate cancer cells through selective light irradiation with blue and orange light respective for SuperNova Green and SuperNova Red activation.

Chapter 4 summarizes this study and giving a future perspective for SuperNova Green application to meet the cutting-edge imaging technique and to achieve a better understanding of biological phenomena.

ABSTRACT

Photosensitizing fluorescent proteins, which generate reactive oxygen species (ROS) upon light irradiation, are useful for spatiotemporal protein inactivation and cell ablation. These give us clues about protein function, intracellular signaling pathways and intercellular interactions. Since ROS generation of photosensitizer is specifically controlled by certain excitation wavelength, utilizing colour variants of photosensitizing protein would allow multi-spatiotemporal control of inactivation. To expand the colour palette of photosensitizing protein, here, I developed SuperNova Green from it red predecessor, SuperNova. SuperNova Green is able to produce ROS spatiotemporally upon blue light irradiation. Based on protein characterization, SuperNova Green produces inconsiderable amount of singlet oxygen and predominantly produce superoxide and its derivatives. I utilized SuperNova Green to specifically inactivate the pleckstrin homology domain of phospholipase C-δ1 and to ablate cancer cells *in vitro*. As a proof of concept for multi-spatiotemporal control of inactivation, I demonstrate that SuperNova Green can be used with its red variant, SuperNova, to perform independent protein inactivation or cell ablation studies in a spatiotemporal manner by selective light irradiation. In conclusion, development of SuperNova Green has expanded the photosensitizing protein toolbox to optogenetically control protein inactivation and cell ablation. As a perspective, SuperNova Green in conjunction with other colour variants would be a relevant tool to be used with other cutting-edge technology, such as super-resolution microscope, to achieve a better understanding of biological phenomena.

ABBREVIATIONS

2-OH-E^+: Dihydroxyethidium

ADPA: Anthracene 4,9 dipropionic acid

AMPA: α-amino-3-hydroxy-5-methyl-4-isoxazolepropionic acid

avGFP: *Aequoria victoria* Green Fluorescent Protein

BRET: Biolimonescence Resonance Energy Transfer

CALI: Chromophore Assissted Light Inactivation

CIB1: Cryptochrome-Interacting Basic-helix-loop-helix

CRISPR: Clustered Regularly Interspaced Short Palindromic Repeats

CRY2: Cryptochrome 2

D_2O: Deuterium oxide

DsRed: *Discosoma sp.* Red

E^+: Ethidium

EDT: 1,2-ethanedithiol

EGFP: Enhanced Green Fluorescent Protein

FlAsH: Fluorescein Arsenical Hairpin

FMN: Flavin mononucleotide

GFP: Green Fluorescent Protein

HE: Hydroethidium

HER-2-ECD: Human epidermal growth factor receptor-2 extracellular domain

LOV domain: Light Oxygen Voltage-sensing domain

MiniSOG: Mini Singlet Oxygen Generator

mRFP: monomeric Red Fluorescent Protein

PH domain: Pleckstrin Homology domain

PLC-δ_1 : Phospholipase C-delta1

ReAsH: Resofurin Arsenical Hairpin

RFP: Red Fluorescent Protein

RNAi: Ribonucleic Acid interference

ROS: Reactive Oxygen Species

SNG: SuperNova Green

SNR: SuperNova Red

SOD: Superoxide dismutase

SOPP: Singlet Oxygen Photosensitizing Protein

STED: Stimulated Emission Depletion

TALEN: Transcription Activator-like Effector Nucleases

TPP^{+}: Triphenylphosphonium

CHAPTER 1: ENGINEERING A MONOMERIC PHOTOSENSITIZER PROTEIN FOR PHOTO-INDUCIBLE PROTEIN INACTIVATION AND CELL ABLATION

1.1 Introduction

Understanding protein function at the molecular, cellular, or even tissue level, has been the focus of wide-range of fields, such as neurobiology, developmental biology, and biomedical engineering. One mostly used method to understand the function of particular protein is to observe the loss-of-function phenotypes. Several methods have been widely used to generate loss-of-function phenotypes e.g. gene knockouts via homologous recombination, CRISPR-Cas9, TALEN; or knockdown method via RNAi, degron, ribozyme, morpholino, inhibitory drugs or function-blocking antibodies.

However, there are some drawbacks of these methods that hamper the elucidation of particular protein function. For instance, conventional gene knockout which deletes or edits target genes of an organism mostly applied at its early developmental stage (Schwartzberg et al., 1989; Thomas and Capecchi, 1987). Thus, gene knockout is inapplicable to elucidate essential protein for development or housekeeping protein function, since loss of those proteins is lethal. Some light- or drug- induced method has been established to enable spatiotemporal control of gene knockout in adult organism (Kiermayer et al., 2007; Schindler et al., 2015). However, still some drawbacks are present. For example, gene knockout is often associated with

compensated expressions of other proteins to overcome the loss of target protein, thus cause no change of phenotype (Hoffman-Kim et al., 2002).

Slightly different from conventional gene knockout, gene knockdown such as RNAi and degron are able to create a loss-of-function phenotype after developmental stage. RNAi works by repressing protein expression at the post-translational step while degron works mostly by initiating protein degradation via ubiquitin-dependent pathway (McCaffrey et al., 2002; Varshavsky, 1991). Applying RNAi with several targeting methods e.g. cell specific antibody or aptamers has improved RNAi specificity to target certain cell/tissue (Kim and Rossi, 2008). However, the time-lag between introduction of RNAi and full loss-of-function phenotype to be achieved depends on the turnover rate of the target protein. Similar with RNAi, even though many approaches have been made to control spatiotemporal activation of degron, at least 30 minutes or several hours are needed to achieve total depletion of protein (Natsume and Kanemaki, 2017). Drugs or function-blocking antibodies may result in fast and direct generation of loss-of-function phenotype but may cause artifacts or side-effects (Wang and Jay, 1996).

To achieve loss-of-function by cell ablation, several methods have been commonly used such as toxin receptor-mediated cell knockout or thermal-induced cell ablation. Specific cell ablation by expressing diphtheria toxin receptor in target cell could be achieved using cell-specific promoter (Saito et al., 2001). Although this method could target selected cell type within tissue or organism, it could not achieve selective ablation on single cell level. Thermal-induced cell ablation via laser or microwave ablation are often used for basic research and cancer treatment (Chu and Dupuy,

2014). However, these approaches would be problematic when applied to deep tissue target since cells located at the surface would be ablated as well. Specific targeting method such as utilizing gold nanoparticle to induce heat generation could achieve better specificity to the target (Moyano and Rotello, 2011). But chemical addition to the system may hamper the spatial approach of target ablation.

Optogenetic method, which utilizes light-induced system with a genetically encoded light-sensitive molecule, has enabled control of living cells and organism behaviour at defined time (milisecond-scale) and space (sub-cellular scale). For example, channelrhodopsin, a light sensitive proton channel which opens ion channels upon blue light irradiation has been widely used to modulate activity of excitable cells such as neuron and cardiomyocytes (Deisseroth, 2011; Nagel et al., 2003). Some other light sensitive proteins which form dimers upon light irradiation, e.g. LOV domain and CRY2, have been employed to control cell signaling pathway by manipulating protein-protein interaction (Rost et al., 2017). In fact, light-induced system to generate loss-of-function phenotype and its development to meet genetically encoded approach has been started since over three decades ago.

1.1.1 Chromophore assisted light inactivation to elucidate protein function

In 1988, Daniel G. Jay first introduced the concept of **chromophore-assisted light inactivation (CALI)**, a method to spatiotemporally inactivate protein by **photosensitizer**, a chemical dye that generates reactive oxygen species (ROS) upon light irradiation (Jay, 1988). First application of CALI was to elucidate the function of Fasciclin I protein in grasshopper embryos. Before the CALI study was performed, Fasciclin I had been known to be expressed on the surface of Ti1 pioneer neurons in

limb bud development. However, the main function of this protein had not been elucidated. The Ti1 pioneer neurons remain in close contact with each other to form single growth cone then extending their axons crossing through epithelia towards the central nervous system, which process is called fasciculation (Figure 1.1.b). Apparently, inactivation of Fasciclin I before this axonal projection by CALI method (Figure 1.1.a) resulted in the separation of two axons, indicating defasciculation (Figure 1.1.c). This result has revealed Fasciclin I essential role in fasciculation of Ti1 pioneer neurons (Jay and Keshishian, 1990).

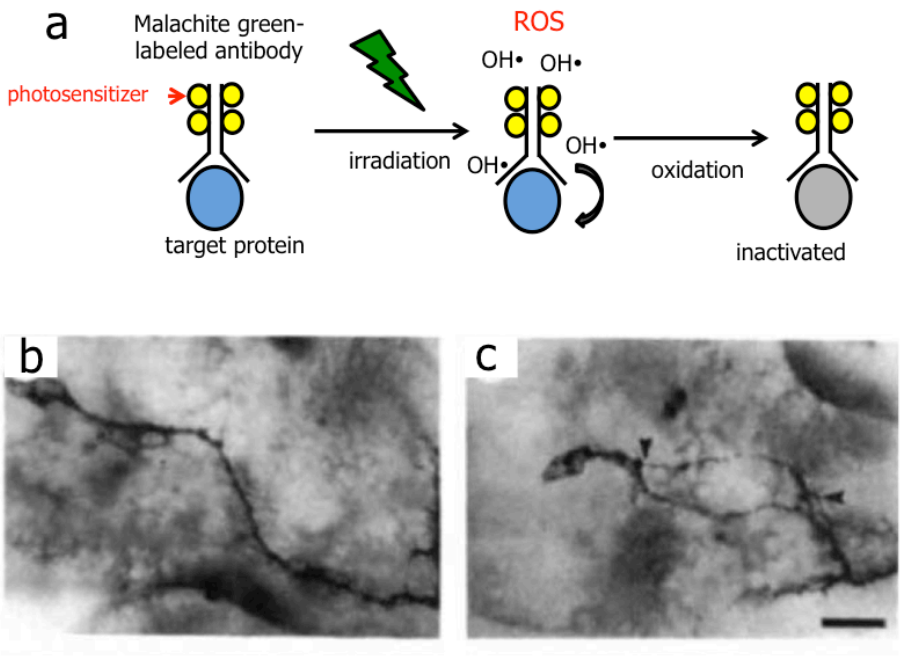

(Jay and Keshishian, 1990)

Figure 1.1. a) Illustration of CALI utilizing malachite green as photosensitizer and antibody to target Fasciclin I. b) Single growth cone of Ti1 sister axons in grasshopper embryo. c) Defaciculation of Ti1 sister axons happens when CALI was applied just before axonal outgrowth of treated embryos. Arrows show point of defasciculation.

This CALI experiment has shown that utilizing targeted photosensitizer and light-induced system could achieve protein inactivation in a very confined area and narrow temporal window. Targeting photosensitizer using laser light could achieve protein

inactivation below subcellular range (nanometer and micrometer scale). Moreover, target inactivation could be achieved just after light irradiation since ROS is highly reactive and immediately oxidize the target molecule. The loss-of-function phenotype will sustain until the next turnover of the target protein.

1.1.1.1 Photosensitization mechanism

The mechanism underlying the ROS production via chromophore excitation (**photosensitization process**) is illustrated in following Jablonski diagram (Figure 1.2). Light irradiation will excite the chromophore to enter excited states, which consists of several states of energy levels. The chromophore will release the energy through non-radiative transition that mostly generates heat then remain in the lowest excited single states for several nanoseconds. In this state, chromophore will release its energy to go back to ground state level through several possible ways: 1) the photosensitizer may emit fluorescence (hvf), 2) transfer its energy to the solvent without emission, 3) cause one electron-reduction of **ground state oxygen ($^3O_2$)**, to produce **superoxide anion ($O_2^{\bullet -}$)** or 4) enter a triplet state via intersystem crossing. Mostly, effective photosensitizers undergo intersystem crossing to produce an excited triplet state, which is relatively long lived before it emits phosphorescence. In the presence of oxygen, triplet state chromophore could produce reactive oxygen through two different mechanisms: 1) via energy transfer to $^3O_2$ then generating **singlet oxygen ($^1O_2$)** which has paired electrons with opposite spins or 2) via electron transfer mechanism to produce $O_2^{\bullet -}$ (Baptista et al., 2017; Foote, 1991; Jacobson et al., 2008).

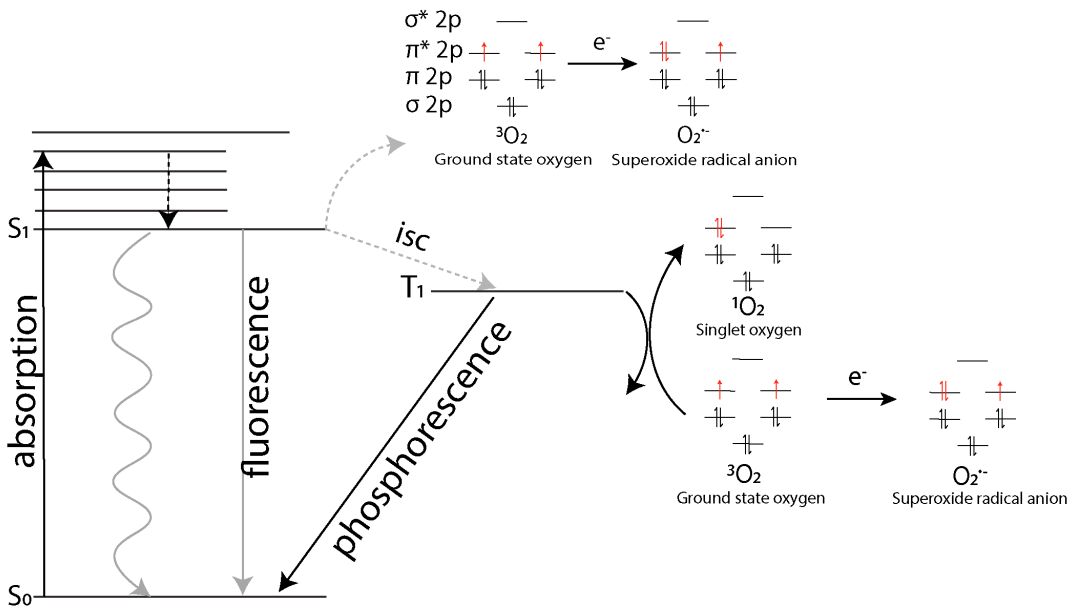

Figure 1.2. Illustration of ROS production mechanism integrated in Jablonski diagram. Upon absorption of a photon, photosensitizer at ground state (S_0) will enter excited state (S_1), or several higher energy level. It may undergo non-radiative transition (black dashed arrow) then release the energy via several pathways: 1) fluorescence emission (gray straight arrow); 2) energy release without fluorescence emission (wavy arrow); 3) $O_2^{\bullet-}$ generation (one electron transfer to ground state oxygen, see red line) or 4) intersystem crossing to enter triplet state. In triplet state, photosensitizer is capable to generate $O_2^{\bullet-}$ or $^1O_2$ (noted the unpaired electron of $^3O_2$ changes its spin, red line).

1.1.1.2 Photosensitizer mechanism to inactivate protein

Free ROS generated by photosensitizer will diffuse to the solvent and attack neighbouring molecules due to their high reactivity. ROS may attack DNA bonds, lipids, or oxidize side chains of amino-acid residues, including histidine, tyrosine, tryptophan, methionine, and cysteine. Those attacks on a protein may result in intramolecular protein structure and function changes. In addition to intramolecular dysfunction, attacked proteins may undergo protein-protein crosslinking or aggregation, leading to intermolecular protein inactivation. In rare cases, ROS may attack peptide bonds and cause peptide fragmentation (Jacobson et al., 2008).

As mentioned in 1.1.1.1, there are different types of ROS that are generated from a photosensitizer, such as $^1O_2$, $O_2^{\bullet-}$ and $O_2^{\bullet-}$ derivatives: **hydrogen peroxide (H_2O_2)** and **hydroxyl radical (OH')**. Different species of ROS has different diffusion range and lifetime in water which ranges from several angstrom to several microns and from 3.5 μs to ~1 ms respectively (details will be discussed in chapter 2). Due to its diffusion capability, it was argued whether ROS would attack non-targeted molecule as well. However, since CALI method requires proximate targeting of photosensitizer to the aimed protein (Figure 1.1a), ROS generated from photosensitizer would likely attack the target before it attacks non-targeted neighbouring molecules (Liao et al., 1995). Due to its light-inducible system and immediate disruption of protein target, CALI had shown its superiority over other methods in the term of spatiotemporal generation of loss-of-function phenotypes.

1.1.1.3 Photosensitizer to induce cell ablation

Since the nature of ROS is toxic and potentially lethal when produced excessively in cells, photosensitizers could induce cell death as well. To activate cell death response effectively, photosensitizers often targeted to mitochondria, chromatin or plasma membrane (Ryumina et al., 2013; Shirmanova et al., 2013b). Similar as protein inactivation, cell specific function within a population could be elucidated by photosensitizer (Kobayashi et al., 2013; Makhijani et al., 2017; Williams et al., 2013). Moreover, many studies have directed the utilization of photosensitizers as photodynamic therapy agent, which kills cancer cells by light irradiation.

1.1.2 Chemical dye-based photosensitizer

The first CALI was demonstrated using malachite green, as the photosensitizing

agent, conjugated to antibody to target the protein of interest. However, most of the CALI application using malachite green was performed by intense laser irradiation because ROS generation of malachite green induced by wide-field irradiation was not sufficient to inactivate protein (Beermann and Jay, 1994). However, effect of high-power laser irradiation itself is already known to cause phototoxicity to the cells (Shah and Jay, 1993). Thus, it was feared that intense irradiation by laser will cause unspecific damage to the whole cell. Moreover, targeting via antibody is considered laborious since first of all, screening must be performed to find the suitable antibody for the target; second, another test must be done to confirm that the antibody does not block the active site of the intended target in order to verify the inactivation is caused by the photosensitizer (Jay and Sakurai, 1999).

Further improvement of targeting method and CALI tools has provided us with less laborious techniques and more efficient ROS generation induced with low power illumination. For example, substituting malachite green with fluorescein produces 50 times higher inactivation efficiency. Several attempts have been made to substitute antibody-targeting techniques with transgenically encoded tag-based techniques. A membrane-permeable fluorescein derivative, 4′,5′-bis(1,3,2-dithioarsolan-2-yl) fluorescein (FlAsH), could bind to the tetracysteine motif, which could be genetically encoded and fused with protein targets. FlAsH was fused to synaptotagmin I, which functions in a post-docking step of vesicle fusion by acting as the major calcium sensor for transmitter release. FlAsH-mediated inactivation of synaptotagmin I, which is essential for transmitter release in neural synapse, decreased transmitter release in *Drosophila* just by visible light illumination from a mercury arc lamp (Marek and Davis, 2002). A stronger ROS generator derived from fluorescein, ReAsH, a red

biarsenical dye, was established later and possesses similar properties to FlAsH, which is membrane permeable and binds to the tetracysteine motif (Adams et al., 2002). However, FlAsH or ReAsH have also been criticized due to their non-specific binding to any cysteine residue of endogenous proteins and their high cytotoxicity due to the necessary addition of EDT, to wash unbound photosensitizers (Hearps et al., 2007; Martin et al., 2005; Stroffekova et al., 2001).

As an alternative to antibody and tetracysteine motif-based targeting, commercially available tags such as SNAP tag or HaloTag have been used to improve targeting method. CALI of SNAP-tag-fluorescein fused to γ-tubulin, has caused a failure in microtubule nucleation and growth, thus leading to cell metaphase arrest (Keppler and Ellenberg, 2009). HaloTag protein, a modified haloalkane dehalogenase, was designed to covalently bind to a variety of haloalkane-containing compounds. Haloalkyl derivatives of fluorescein and Ru(II)tris(bipyridyl) were tested for use in combination with HaloTag and specific CALI could be achieved by fusing target proteins with photosensitizer-labelled HaloTag. Later, diAc-eosin derived from eosin was synthetized to be linked with HaloTag7, a new HaloTag mutant, with superior ability to form covalent bonds with ligands. Using HaloTag7-diAc-eosin to specifically target Aurora-B has been shown to stop cell division, resulting in multinuclear structure formation after mitosis (Takemoto et al., 2011). To date, eosin is considered to be the most powerful photosensitizing agent that has been applied for CALI purposes in mammalian cells and *in vivo*. Recently, CALI using eosin was demonstrated to manipulate animal behaviour by inactivating synaptic GluA1 AMPA receptors to erase fear memory in mice (Takemoto et al., 2016).

1.1.3 Genetically encoded photosensitizer

Although targeting method for chemical dye based-CALI has been improved to avoid non-specific inactivation, the exogenous addition of labelling reagents is still needed while penetration of which may be an obstacle in thick specimens with multiple cell layers. In addition to that, unbound chromophore may affect non-specific inactivation. Genetically encoded fluorescent proteins, such as EGFP, have been well known as being easily fused with protein targets or subcellular localization tags. Since any excited molecules have potential to undergo photosensitization, EGFP chromophore is potentially could react with ground state oxygen or other substrate to generate ROS.

1.1.3.1 EGFP

The first approach to photosensitizing using EGFP was performed in 1998 by Surrey and colleagues. They showed that EGFP could inactivate beta-galactosidase with the energy doses required being almost same as for malachite green (Surrey et al., 1998). Later, EGFP was used to inactivate alpha actinin, resulting in the detachment of stress fibres from focal adhesions and causing retraction of stress fibres. However, the approximate light dose used for CALI utilizing EGFP was at least 10^6 times higher (~1GW/cm^2) than for typical confocal imaging, which caused phototoxicity to living cells (Rajfur et al., 2002). Since EGFP chromophore is located at the center of encapsulating beta barrel structure, ratio of escaped ROS to those trapped in the beta barrel affects the effectiveness of ROS generation by EGFP. It was speculated that an effective photosensitizing fluorescent protein would enables large amount of ROS to escape the beta barrel thus ROS become more likely to reach the protein target (McLean et al., 2009).

1.1.3.2 KillerRed

To find the most effective photosensitizing fluorescent protein, Bulina and colleagues (2006) performed screening on GFP homologs derived from anthozoan, hydrozoan and copepod based on their phototoxic effects on *E. coli* cells. As the result, they found KillerRed, a mutant derived from anthomedusa chromoprotein, to have phototoxic effect thus makes it the first effective genetically encoded photosensitizer. The unique property of KillerRed that makes it different to other fluorescent protein is the formation of pore inside beta barrel contained eight water molecules that interconnected by hydrogen bonds from chromophore to the opening of beta barrel (Figure 1.3a). Several hypotheses have been made regarding the mechanism underlying effective generation of ROS by KillerRed. The first speculation is the water filled channel enables free accession of oxygen molecules to the chromophore as well as diffusion of ROS to outside of the beta barrel. Second speculation is the chain of water molecules may serve as electron wires that conducts electron transfer generated by excited chromophores to external molecules, resulting in ROS generation near the opening of the beta barrel (Carpentier et al., 2009; Pletnev et al., 2009).

When compared to EGFP, KillerRed resulted in 100% beta-galactosidase inactivation upon 25 min of irradiation with 1 W/cm^2 white light, while EGFP only resulted in 40% inactivation upon irradiation with sevenfold more light power. Compared to ReAsH, KillerRed is only threefold less efficient (Bulina et al., 2006). After its establishment, KillerRed has shown its applicability for *in vitro* CALI of aquaporin isoforms, cofilin (Figure 1.3b), and GRASP 55/65 (proteins that essential for golgi compartmentalization) (Baumgart et al., 2012; Jarvela and Linstedt, 2014; Vitriol et

al., 2013). Moreover, KillerRed has also been demonstrated to be able to induce death of heart, muscle, neuron and tumour cells *in vivo* (Kobayashi et al., 2013; Shirmanova et al., 2015; Teh and Korzh, 2014). In conclusion, development of KillerRed has provided us an effective and specific ROS generation with a genetically labelling method.

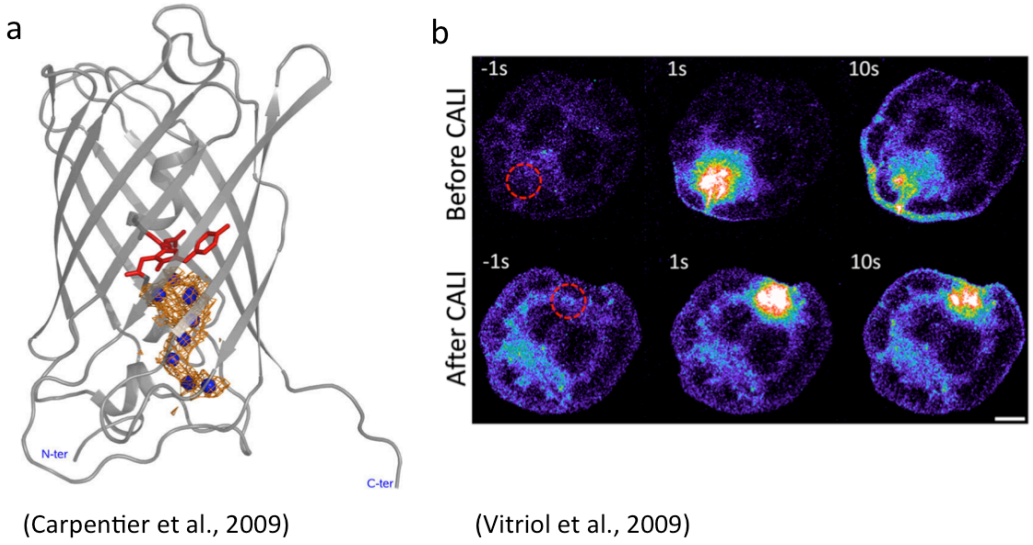

(Carpentier et al., 2009) (Vitriol et al., 2009)

Figure 1.3. X-ray crystallographic structure of KillerRed (left). Red colour shows chromophore in the center of beta barrel that connected by eight water molecules (blue) to the opening of beta barrel (Carpentier et al., 2009). Right figure shows fluorescence of PA-GFP-actin before and after CALI of cofilin on red circular region. CALI of cofilin decreased actin filament turnover.

Though KillerRed has shown its usefulness, it was reported to have a dimerization tendency when expressed at high concentration in cells. This dimeric property hampers subcellular localization (Bulina et al., 2006) or affects cell division (Takemoto et al., 2013a). SuperNova, a monomeric variant of KillerRed, was developed and described to possess superior properties as a fusion partner with signal peptides or localized proteins (Takemoto et al., 2013a). SuperNova has been

demonstrated to promote CALI of cofilin and F-actin (Kim et al., 2015) , as well as *in vitro* cell ablation (Takemoto et al., 2013a).

1.1.3.3 Genetically encoded photosensitizer colour variants and their prospective application

Development of fluorescent protein colour variants has enabled multi-colour imaging of different targets in a single cell or organism by separating excitation and emission wavelength. When similar concept is applied to photosensitizer that is activated by certain excitation wavelength as well, combination of several colours of photosensitizer would enable multi-targeting different protein/cell of interests. This is an expanded concept of CALI, here I call "multi-CALI", that would allow selectively inactivate different proteins within single cells using activating light which can be controlled precisely in space and time with subcellular resolution (Figure 1.4c). In an organism, this concept would allow selective ablation of two different cell population in spatial and temporally controlled manner (Sarkisyan et al., 2015; Williams et al., 2013).

Derived from KillerRed and SuperNova, colour variants of genetically encoded photosensitizers have been developed; KillerOrange and mKillerOrange (dimeric and monomeric orange variant of KillerRed respectively) (Sarkisyan et al., 2015) and a dimeric green variant of KillerRed (De Rosny and Carpentier, 2012). In 2011, a monomeric green genetically encoded photosensitizer called miniSOG (miniSingletOxygenGenerator) was developed from the LOV domain of *Arabidopsis thaliana* Phototropin 2 (*AtPhot2*). miniSOG contained FMN (flavin mononucleotide) as its chromophore (Shu et al., 2011). Several improved variants of miniSOG such as

SOPP (Singlet Oxygen Photosensitizing Protein) (Westberg et al., 2015), SOPP2, SOPP3 (Westberg et al., 2017) and miniSOG2 (Makhijani et al., 2017) has been described to produce more $^1O_2$ compared to the original miniSOG. However, the ROS generation of miniSOG and its variants is dependent on the FMN concentration (Ryumina et al., 2013). In contrast to miniSOG, KillerRed based variants do not depend of FMN concentration for phototoxicity since they have spontaneously forming GFP-like chromophores (Carpentier et al., 2009). Therefore, in certain applications where the environment lacks of FMN, KillerRed based variants are preferable**.**

1.2 Purpose and significance

Based on the multi-CALI purpose and to overcome the drawbacks of established green variant of genetically encoded photosensitizer, this study was aimed to develop a green successor of SuperNova (hereafter called SuperNova Red/SNR (Figure 1.4b). Following the development, protein characterization was performed to evaluate the green variant of SNR physicochemical properties.

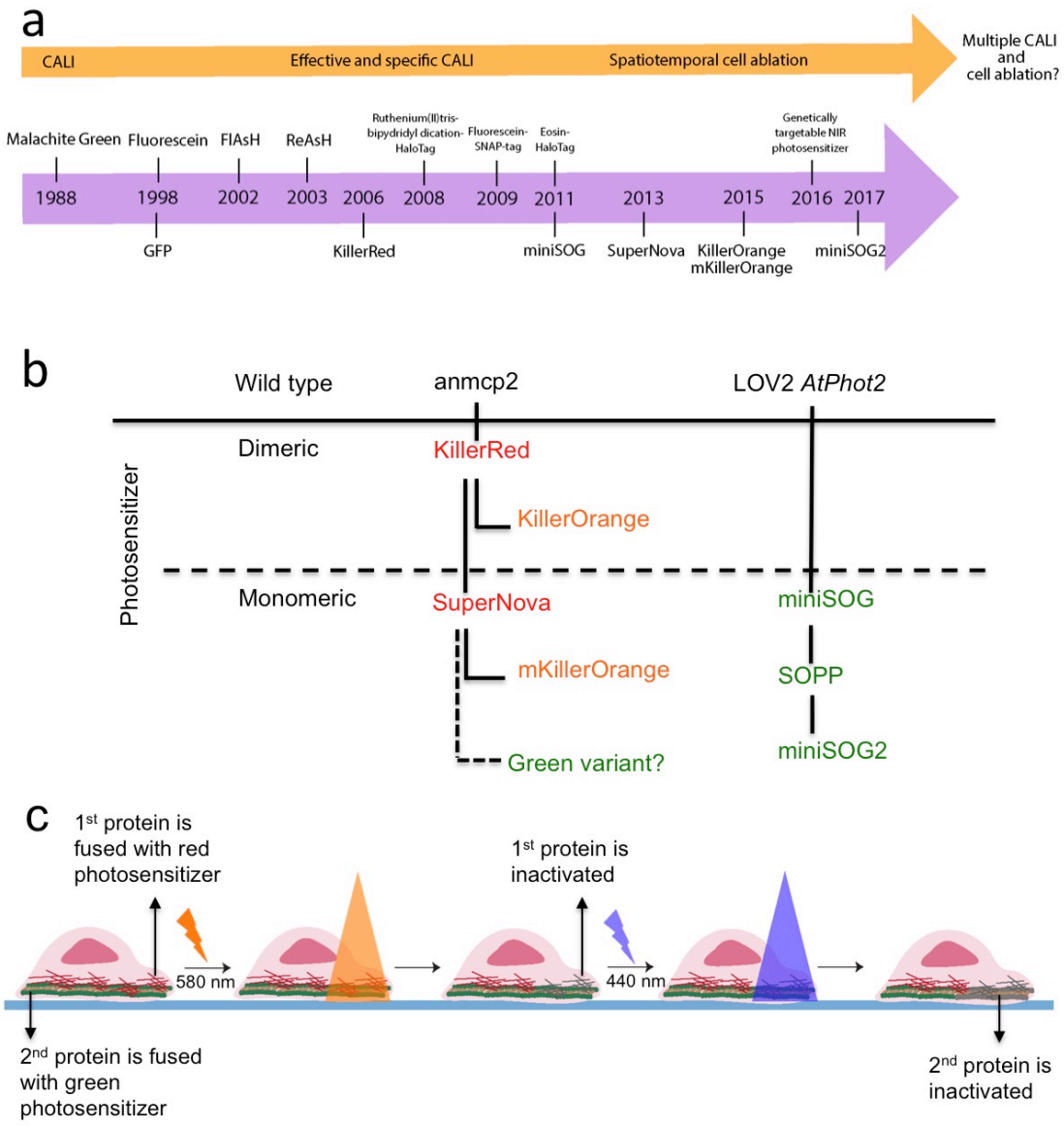

Figure 1.4. a) Development of CALI tools timeline (purple) and its trend of application (orange). b) Currently available genetically encoded photosensitizer. Development of the green monomeric version of KillerRed-based variant is the main focus of this study. c) Illustration of multi-CALI. The idea is to target two different proteins with two colour of photosensitizer (green and red colour). Irradiation with 580 nm and 440 nm would result in inactivation of protein fused with red and green photosensitizer respectively in an independent manner.

1.3 Materials and methods

1.3.1 Gene construction and screening process

To establish green variant of SNR, Y66W and V44A point mutation was introduced to SNR/pRSET$_B$ using inverse PCR method. Direct mutagenesis was performed based on previous study (De Rosny and Carpentier, 2012; Sarkisyan et al., 2015).

For protein characterization, several vectors containing other photosensitizer proteins are constructed for this study. V44A-KillerRed was established by introducing V44A mutation to KillerRed-pRSET$_B$ plasmid using inverse PCR method. miniSOG was cloned from miniSOG-C1 (Addgene #54821) plasmid into pRSET$_B$ using the *Bam*HI-*Eco*RI restriction site.

To check monomeric property of green variant of SNR and to compare monomeric property of this variant with its predescessors, several mammalian expression vectors expressing photosensitizer proteins tagged to target protein or localization signal were established. PCR-amplified green variant of SNR, V44A-KillerRed and KillerRed were cloned into 2xCOXVIII-SNR/pcDNA3.1 by *Bam*HI and *Eco*RI restriction enzyme digestion. Fusion with vimentin was performed by replacing Kohinoor in Vimentin-Kohinoor/pcDNA3.1 (Addgene #67772) with photosensitizer proteins using *Bam*HI and *Eco*RI restriction enzyme digestion. Fibrillarin constructs were made by replacing SNR in SNRΔ11-Fibrillarin/pcDNA3.1 with KillerRed, KillerRed V44A and green variant of SNR using the *Hin*dIII/*Bam*HI restriction site. Lyn, H2B and LifeAct construct were made by replacing OeNL in Lyn-OeNL/pcDNA3.1 (Addgene #89528), Nano-lantern-H2B/pcDNA3 (Addgene #51971) and Kohinoor-Actin/pcDNA3.1 (Addgene #67776) with green variant of SNR at the *Bam*HI-*Eco*RI

restriction site. All oligonucleotides using to ampify cDNA fragments are all listed in Supplementary data: Table S1.

Plasmids were transformed into XL 10 Gold *E. coli* cells (Agilent Technologies) using the heat shock transformation at 42^{o} C for 45 seconds. Grown colonies were picked and cultured in 1.5 LB medium containing 0.1 mg/mL carbenicillin then processed for plasmid purification. DNA sequence of mutants was confirmed by dye terminator dye sequencing using Big Dye Terminator v1.1 Sequencing Kit (Applied Biosystem).

1.3.2 Protein purification

Purified pRSET$_B$ containing gene encoding protein tagged with N-terminal polyhistidine tags were transformed into JM109(DE3) (Promega) by heat shock transformation at 42^{o} C for 45 seconds. Transformants were then plated onto agar plates containing 0.1 mg/mL carbenicillin. Colonies were cultured in 200 mL LB media containing 0.1 mg/mL carbenicillin at 23^{o}C with gentle shaking at 80 rpm for 4 days. Polyhistidine-tagged proteins were purified by Ni-NTA agarose (Qiagen) chromatography then eluted using 200 mM imidazole in TN buffer (10 mM Tris-HCl pH 8, 150 mM NaCl). Eluted protein was processed to buffer exchange chromatography using a PD-10 column (GE Healthcare). Final elution was diluted in 50 mM HEPES-KOH (pH 7.4)

1.3.3 Spectroscopy

Protein concentration was measured using alkaline denaturation method. Protein purity was confirmed using SDS-PAGE Analysis. Absorption spectra were measured

on a V630-Bio spectrophotometer (JASCO). The absorbance peak was used for molar extinction measurement. Molar extinction coefficient was defined by following equation $\varepsilon=A/c$ where ε as molar extinction coefficient at absorbance peak, A as absorption at the peak wavelength, and c as protein concentration.

For fluorescence spectrum measurement, the protein was diluted until absorption at the peak wavelength was 0.05. Fluorescence spectrum was measured using F7000 fluorescence spectrophotometer (Hitachi). Emission spectrum was measured using 380 nm, 400 nm, 420 nm, 440 nm, 480 nm, and 510 nm as excitation wavelengths. Meanwhile 490, 510, 540, 560, 580, 610 nm were used for the emission wavelengths. To measure the quantum yield, protein was diluted to 5 μM. Absolute quantum yield of protein was measured using Hamamatsu Photonics C9920-01 spectrometer (Hamamatsu Photonics) at 610 nm and 510 nm for original SuperNova and new colour variant mutant respectively.

1.3.4 Size exclusion chromatography

Size exclusion chromatography was performed with Superdex75 100/300GL column (GE Healthcare) with ÄKTA explorer 10S (GE Healthcare). 1 mL of 10 μM protein was injected to the column then eluted with 10 mM HEPES 100 mM NaCl, pH 7.2. Elution was performed at 1 ml/min.

1.3.5 Photobleaching assay

Green variant of SNR and EGFP 10 μM protein solution was placed at silicone made microwell (1-2 mm in diameter) covered with cover glass. Protein solutions were exposed to 17 W/cm^2 of 447/60-25 nm (Brightline) and 475/42-25 nm (Brightline)

excitation light for green variant of SNR and EGFP respectively with mercury arc lamp as light source. Images were taken for every 10 mins for 8 hours. Fluorescence intensity from images was measured using Metamorph software (Molecular Devices). Curve fitting and determination of $t_{1/2}$ was done using Origin Software (OriginLab).

1.3.6 Cell culture, transfection and localization imaging

HeLa cells (RIKEN BRC) and HEK293T cells (ATCC) were cultured with DMEM-F12 with phenol red (ThermoFisher Scientific) supplemented with 10% FBS (Biowest). Cells were incubated at 37^{o}C with 5% CO_2. For subculture, cells were washed with sterile PBS and dissociated with trypsin. Cells subjected to plasmid transfection were seeded on 3 mm glass bottom dish and DNA transfection was done with either calcium phosphate method or using Lipofectamine 2000 (Invitrogen, Carlsbad, California). For all live imaging experiment performed in this thesis, after 48 hours of transfection, medium was changed to DMEM/F12 without phenol red (ThermoFisher Scientific) added with 100 µg/mL penicillin/streptomycin (ThermoFisher Scientific). Imaging of subcellular localization was done using confocal microscope (FV1000, Olympus) using a 60X NA 1.4 oil immersion objective. Images were taken using 450 nm and 580 nm multi-Argon ion lasers.

1.4 Results and discussion

1.4.1 Establishment of green variant of SuperNova Red

It is well known that in order to emit red fluorescent, chromophore has to undergo maturation to extend the π-conjugation in p-hydroxybenzelidene imidazolinone to acylimine bond (shown by arrow, Figure 1.5). In other words, red fluorescent protein such as DsRed must undergo blue/green emitting state before matured to red emitting state (Tubbs et al., 2005). KillerRed possesses similar chromophore structure as DsRed (Figure 1.5). Thus, prevention of red chromophore maturation must generate green/blue variant. Introduction of V44A mutation to KillerRed (KillerRed-V44A) (De Rosny and Carpentier, 2012) generated a green colour variant of KillerRed that was reported to have no photosensitizing property. However, changing chromophore structure may result in different chromophore environment that lead to different photosensitizing ability. For instance, KillerRed and KillerRed-V44A has tyrosine based chromophore that results in protonated and deprotonated state of chromophore as characterized in avGFP (De Rosny and Carpentier, 2012). It was speculated that changes of state affects the photosensitizing ability of KillerRed. On the other hand, absence of hydroxyl group in tryptophan-based chromophore as shown in KillerOrange eliminates that possibility.

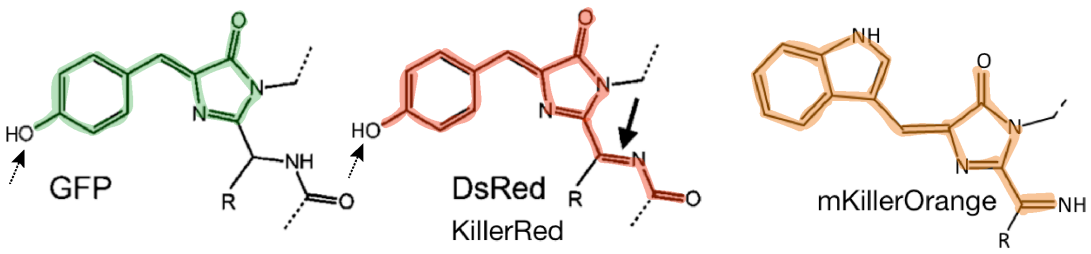

Figure 1.5. Chromophore structure of GFP, DsRed, KillerRed and KillerOrange. Tyrosine based chromophore posseses hydroxyl group (dashed arrow). Extension of acylimine bond (arrow) creates red-shited chromophore.

Following hypothesis above, first, Y66W mutation was introduced into SNR to change the tyrosine-based chromophore to tryptophan-based chromophore. This mutant generated the orange variant of SNR, known as mKillerOrange (Sarkisyan et al., 2015), which had absorbance peak at 453 nm with shoulder at 510 nm. Further, I introduced V44A mutation into mKillerOrange and obtained new colour variant which has absorption peak at 437 nm with a smaller shoulder at 510 nm (Figure 1.6c). When illuminated with UV light, this variant emits green colour thus this variant is called SuperNova Green (hereafter is called SNG) (Figure 1.6.a). As result of spectroscopic analysis, SNG shows dual excitation/emission at 440/510 nm and 480/560 nm respectively with molar extinction coefficient 28,000 $M^{-1}cm^{-1}$ and absolute fluorescence quantum yield of 0.23 (Figure 1.6d, Table 1.1).

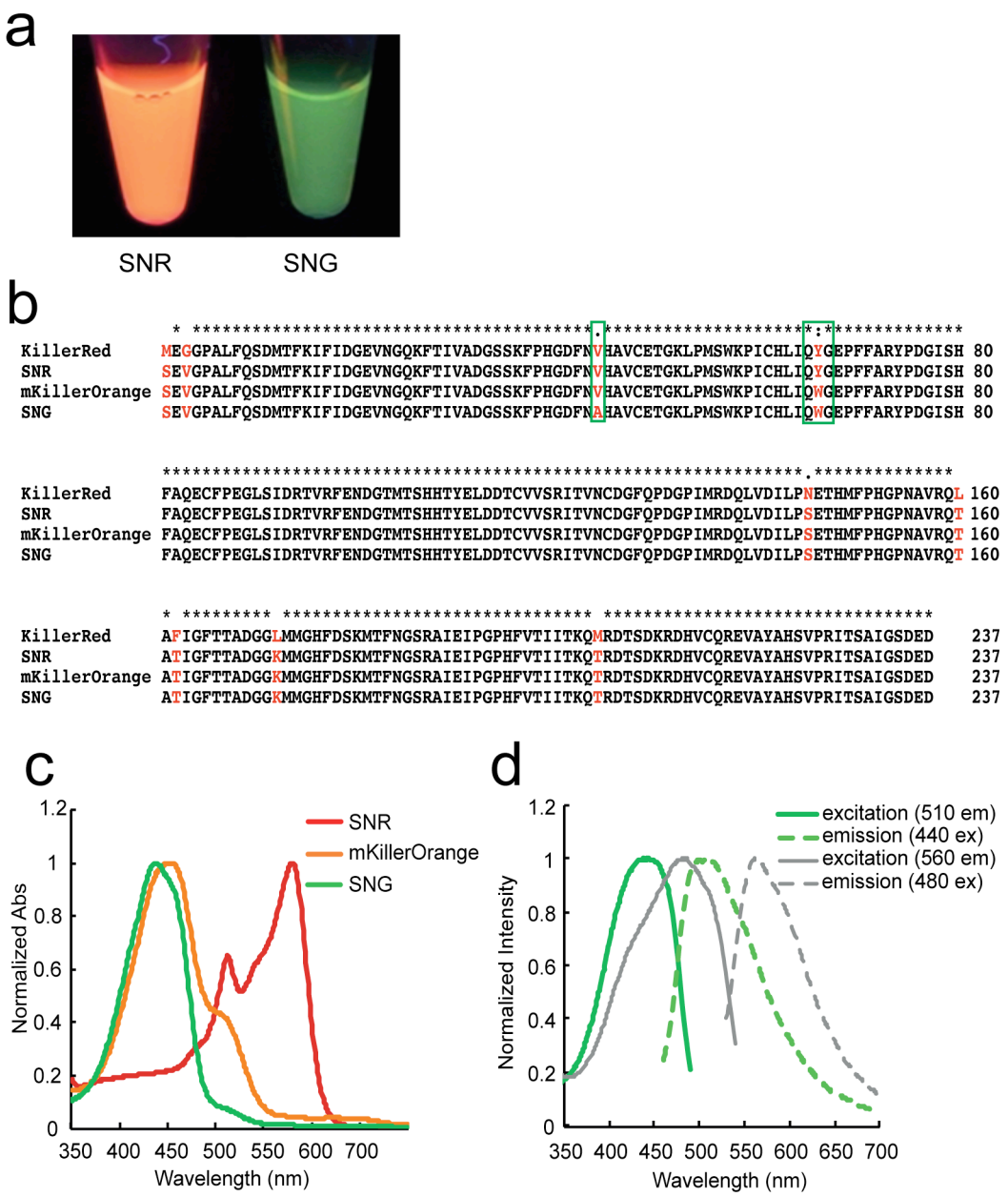

Figure 1.6. Establishment of SNG. a) Protein solution of SNR and SNG illuminated by UV light. b) SNG sequence compared to KillerRed, SNR and mKillerOrange. Green box highlights the V44A mutation and tryptophan-based chromophore owned by SNG. c) Absorption specta of SNR, SNG and mKillerOrange shows blue shifted peak of SNG with a smaller shoulder ~510 nm compared to mKillerOrange spectrum. d) Excitation (solid line) and emission (dashed line) spectra of SNG.

Table 1.1. Protein characteristics of SNR and SNG

Protein	Abs peak (nm)	λ_{ex}(nm)	λ_{em}(nm)	ε ($M^{-1}cm^{-1}$)	QY
SNR	579	579	610	33,600	0.3
SNG	437	440	510	28,000	0.23
		480	560		

1.4.2 Analysis of dual excitation and emission of SNG

Double excitation and emission coming from SNG (Figure 1.6d) was speculated to be the result of the matured orange chromophore and intermediate green chromophore. There is also a chance that dual excitation and emission of SNG coming from single SNG molecule, not from matured and intermediate form of chromophore in a population. However, to test this, single molecule spectrum analysis is needed. Due to its complexity, only analysis of a population was performed.

Rosny and Carpentier (2012) found two alternative conformations of E68 side chain in A44-KillerRed. One of which was in a catalytic position to promote green to red maturation similar to S69 in DsRed by catalyzing acylimine bond formation (Tubbs et al., 2005) while the other conformation was an inactive form. Moreover, they also found two conformations of I64 in V44A-KillerRed that results from the existance and non-existance of double acylimine bond in protein fraction (shown in Figure 1.7).

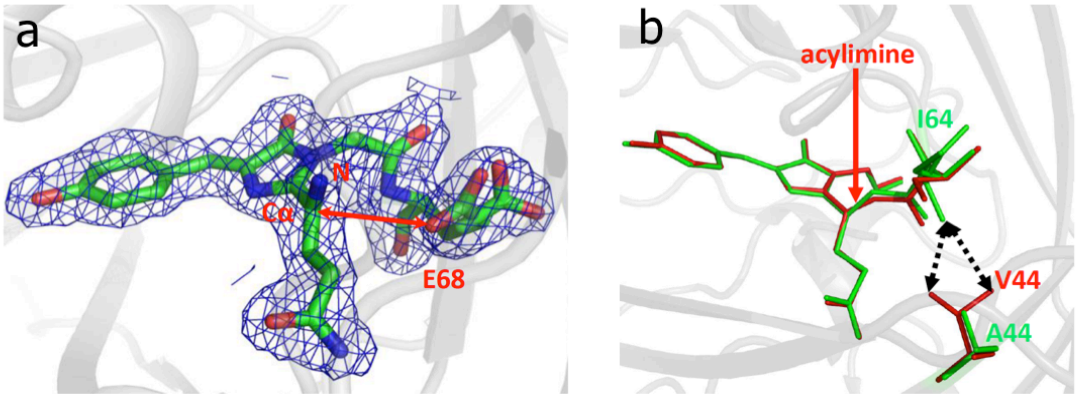

Rosny and Carpentier (2012)

Figure 1.7. a) Double conformation of E68 in A44-KillerRed. The active conformation promotes formation of acylimine bond of the pointed Cα (red arrow). b) Red and green represents KillerRed and KillerRed-V44A chromophore respectively. V44A relaxes I64 conformation resulted in two alternative conformations of I64.

To test the presence of two maturation states of the chromophore, fluorescence emission of SNG and mKillerOrange from 0.05 μM protein solution was measured under the same measurement condition. Excitation of mKillerOrange at 440 and 510 nm both gave an orange emission peak ~560 nm (Figure 1.8a), while excitation of SNG at 440 nm gave green emission peak ~500 nm and excitation at 510 nm resulted in orange emission peak (Figure 1.8b). This result suggests that the V44A mutation creates two forms of chromophore in SNG protein solution: the matured form of the orange chromophore and the intermediate green chromophore.

SNG excited with 440 nm and 510 gave different fluorescence emission intensity. The orange emission was 60% lower than the green emission. On the other hand, mKillerOrange excited with 510 nm showed greater fluorescence emission intensity than excitation at 440 nm. Therefore, mKillerOrange chromophore matures to orange chromophore completely while V44A mutation presence in SNG prevent maturation of some of the protein fraction thus produces green emission.

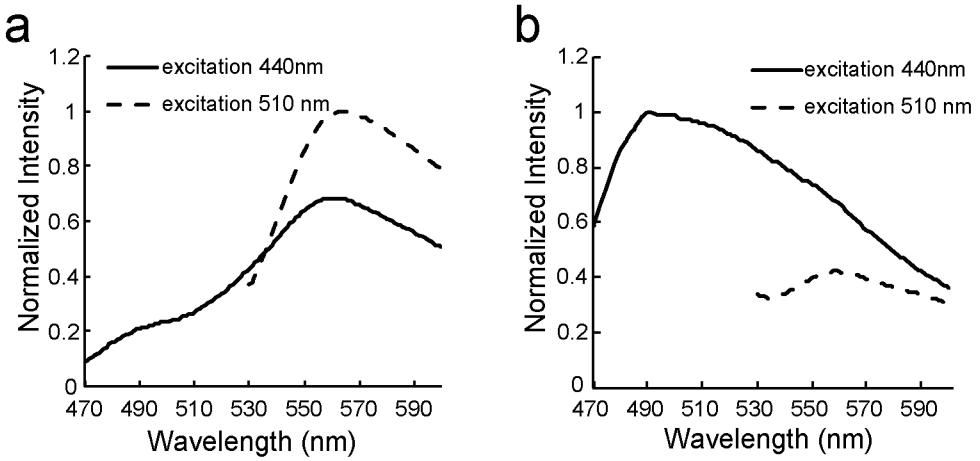

Figure 1.8. mKillerOrange (a) and SNG (b) emission spectra when excited with 440 nm (solid line) and 510 nm (dashed line).

Since the 440 nm excitation corresponds for the green emission which enables better spectral separation compared to orange emission when used concomitantly with red variant, hereafter 440 nm is used SNG excitation wavelength. Furthermore, unlike mKillerOrange, 510 nm excitation did not cause significant ROS generation of SNG (further shown in Figure 4.1).

An attempt to obtain another green emitting variant from mKillerOrange were done. Several site random mutageneses were introduced on several amino acids located near the chromophore (Supplementary data 1). Some of the mutation has shown to produce green emission such as Q65T and E68Q (Supplementary figure S1). Based on previous study, E68Q mutant was incapable to generate ROS (Pletnev et al., 2009). Although this study has not performed further characterization of those mutants, these data would be useful for further improvement of SNG or crystal structure analysis. So far, SNG is still the best green variant of SNR and also capables to generate ROS.

1.4.3 Photobleaching property of SNG

As part of fluorescent protein characterization, $\tau_{1/2}$ of fluorescence photobleaching is commonly used as a standard to compare photostability between fluorescent proteins. For long-term imaging purpose, slow photobleaching property is preferable. But for photosensitizer, there is correlation between photobleaching and ROS production. For KillerRed, many applications and study correlated rapid bleaching with ROS production that result in amino acid side chain destruction at position 65 and 66 (Pletnev et al., 2009). For miniSOG, a positive correlation was found between photobleaching and increasing of $^1O_2$ amount that produced upon prolonged light irradiation (Ruiz-González et al., 2013).

In this study, photobleaching of SNG was investigated by irradiating 10 μM protein solution with 440 nm excitation light. The bleaching rate of SNG was compared to 10 μM EGFP solution excited with 480 nm light at the same power density. The result showed SNG bleaches faster than EGFP with SNG $\tau_{1/2}$ equals to 10 mins and EGFP $\tau_{1/2}$ equals to 70 mins (Figure 1.9).

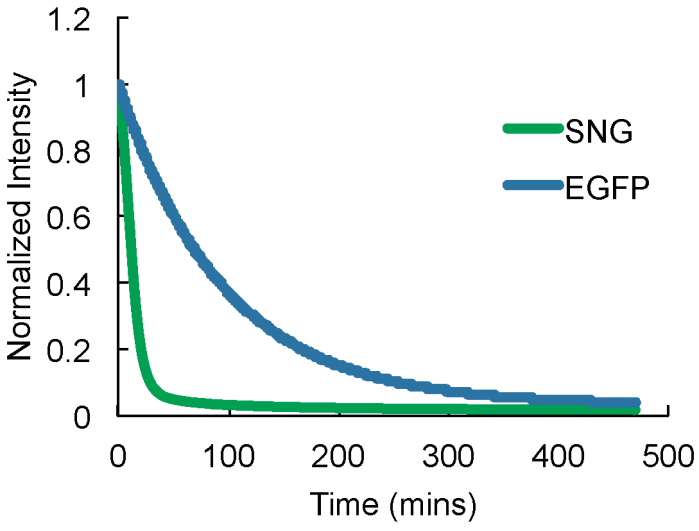

Figure 1.9. Photobleaching curve of SNG and EGFP.

Although correlation between photobleaching and ROS production of SNG is not longer discussed in this study, fast photobleaching of SNG may reflect ROS generation property that possibly higher in SNG compared to EGFP. ROS generation of SNG compared to EGFP is further directly assessed in mammalian cell (see chapter 2).

1.4.4 Monomeric property of SNG

It is widely known that oligomerization of genetically encoded tag such as fluorescent protein may affect dislocalization or aggregates formation thus create undesirable background or observational error in living cells. Almost every new established protein are engineered to its monomeric configuration, for instance, DsRed to mRFP1 and mFruits family (mCherry, mOrange and mRaspberry), and in photosensitizer protein: KillerRed to SNR (Campbell et al., 2002; Shaner et al., 2004; Takemoto et al., 2013a). Although engineering of SNG still mainly consists of SNR amino acid, especially those located at the surface of beta barrel, still I need to confirm the oligomeric status of SNG. Using *in vitro* gel filtration chromatography at 10 μM protein solution, SNG maintains the same monomeric property as its parental protein, SNR (Figure 1.10) and a standard monomeric fluorescent protein, mCherry. Similar to data shown in (Takemoto et al., 2013a), based on protein marker position, our data shows SNR, SNG and mCherry sizes somehow shifted to > 29 kDa (when expected size is ~27 – 29 kDa). However, SNR monomericity has been confirmed using ultracentrifugation method. Thus, I concluded that SNG maintains SNR monomeric property. Meanwhile, KillerRed showed peak near to 75 kDa meaning that oligomerization occurs at 10 μM protein concentration.

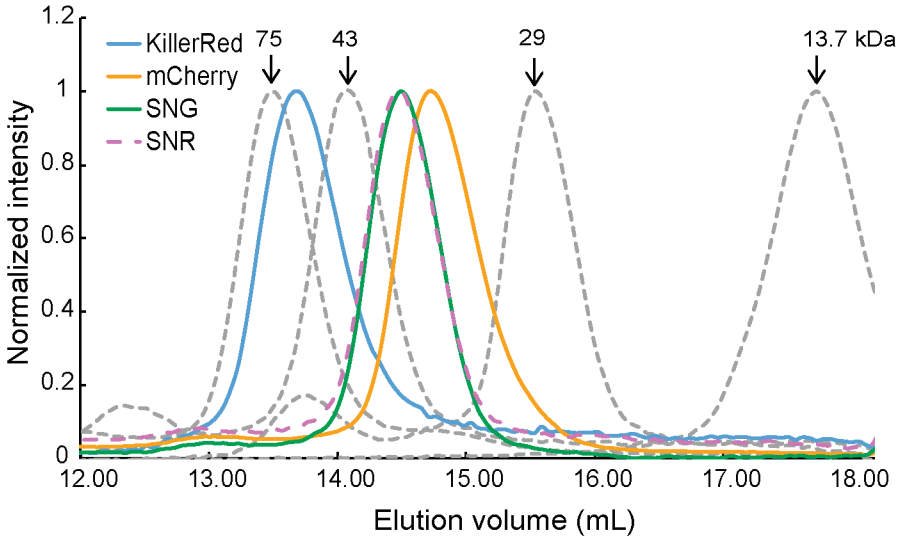

Figure 1.10. Gel chromatography result. KillerRed (~29 kDa) formed a dimer at 10 uM protein concentration meanwhile SNG and SNR elute as monomers together with mCherry as monomer control. 75 kDa (Canalbumin), 43 kDa (Ovalbumin), 29 kDa (Carbonic anhydrase) and 13.5 kDa (Ribonuclease A) were used as marker (dashed grey line).

To further evaluate SNG monomeric property in mammalian cells, SNG was fused to fibrillarin and vimentin in HeLa cells (Figure 1.11a-h). KillerRed and KillerRed-V44A fusions to fibrillarin, a nucleolar protein, showed fluorescence leakage on cytoplasm and the whole nucleus, while SNR and SNG specifically highlighted nucleolus structure. KillerRed and KillerRed-V44A fusion to vimentin, an intermediate filament, showed aggregation around nucleus, whereas the monomeric SNG and SNR both showed proper filament structure. Furthermore, to test SNG ability as subcellular/protein tag, SNG was fused with several proteins and subcellular localization signals e.g. lyn (plasma membrane), histone 2B (nucleus), actin (cytoskeleton) and two tandem copies of mitochondrial localization signal

(mitochondria). As shown in Figure 1.11i-l, SNG highlighted those structures without observable aggregation or abnormalities.

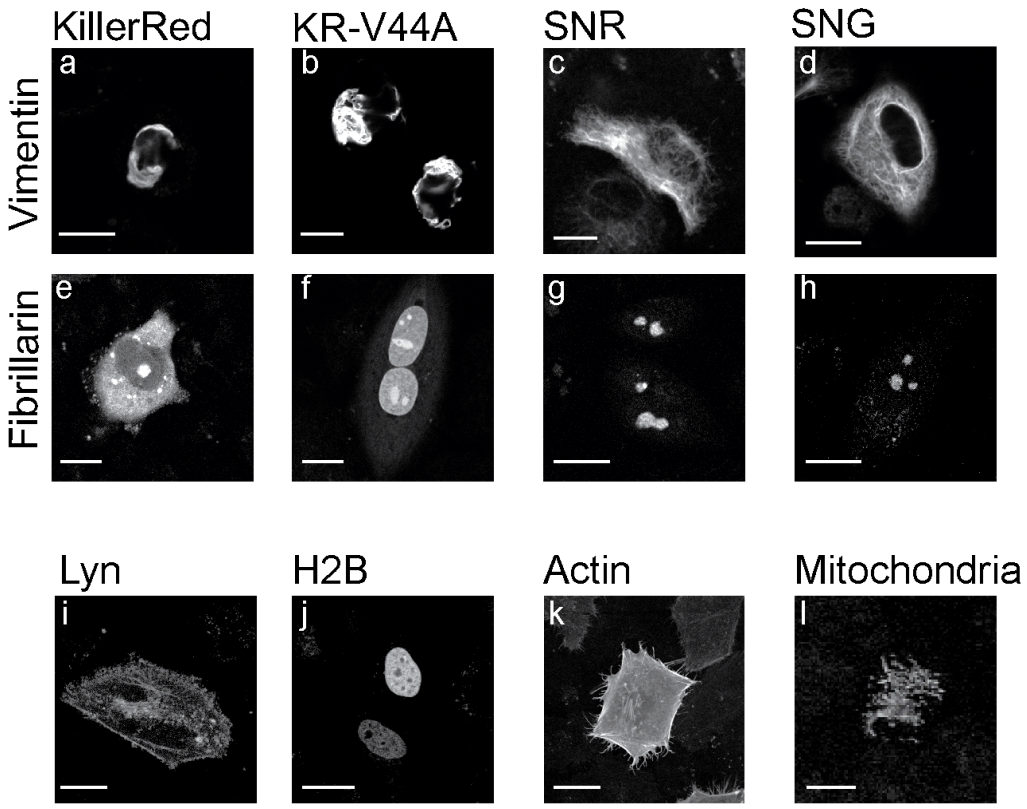

Figure 1.11. SNG monomeric property in mammalian cell. Comparison of KillerRed, KillerRed V44A (KR-V44A), SNR and SNG fused with Vimentin and Fibrillarin of HeLa cells (scale bar: 20 μm) (a-h). SNR and SNG showed correct localization to all target proteins tested meanwhile KillerRed and KR-V44A did not. (i-l) fusion of SNG to lyn, histone 2B, actin and tandem copies of mitochondria localization signal. Scale bar=20 μm.

1.5 Summary

I have successfully generated the green variant of SuperNova Red (SNR) called SuperNova Green (SNG) that possesses tryptophan-based chromophore and V44A mutation. SNG has double excitation and emission spectra that resulted from intermediate green and matured orange fraction. Emission intensity measurement indicated that the green intermediate form dominates the SNG fraction. As protein

characterization result, SNG is shown to photobleach faster than EGFP and maintains its predescessors, SNR, monomeric property. Fast photobleaching of SNG may correlate with the ROS generation property. Furthermore, monomeric property of SNG provides advantages to tag protein target or proper localization in mammalian cells.

CHAPTER 2: PHOTOSENSITIZATION PROPERTY OF SUPERNOVA GREEN

2.1 Introduction

2.1.1 Diverse type of ROS and their individual properties

As mentioned in subchapter 1.1.2, photosensitization reaction would generate ROS via electron transfer to $^3O_2$ to generate $O_2^{\bullet-}$ or energy transfer to $^3O_2$ to produce $^1O_2$ (Foote, 1991). Based on measurement in water, $^1O_2$ diffusion coefficient is ~1000 $\mu m^2 s^{-1}$ with 3 μs lifetime in water and diffusion distances of 0.1 μm (Jacobson et al., 2008). Diffusion rate or range of superoxide anion radical ($O_2^{\bullet-}$) is not yet assessed due to its instability and spontaneous dismutation process (D'Autréaux and Toledano, 2007). Dismutation reaction of $O_2^{\bullet-}$ generates hydrogen peroxide (H_2O_2) which has relatively longer lifetime ~1,000 μs with several μm diffusion range (Winterbourn, 2008). Electron exchange between $O_2^{\bullet-}$ and H_2O_2, via Haber-Weiss reaction would result in highly reactive and unspecific species, hydroxyl radical ($OH^{\bullet}$), which may diffuse over ~10^{-3} μm and has 10^{-3} μs lifetime in water (Liao et al., 1994) (Figure 2.1).

However, based on the data collected on the currently available CALI tools, result of their half radius of damage measurement does not always agree with ROS diffusion in solution. For example, fluorescein which generates $^1O_2$ was measured to have half radius damage ~4 nm, which is quite different to the expected diffusion range of $^1O_2$ in water. Therefore, there are other factors that may affect ROS approachability to the target such the abundance of scavenging molecules surrounding the chromophores.

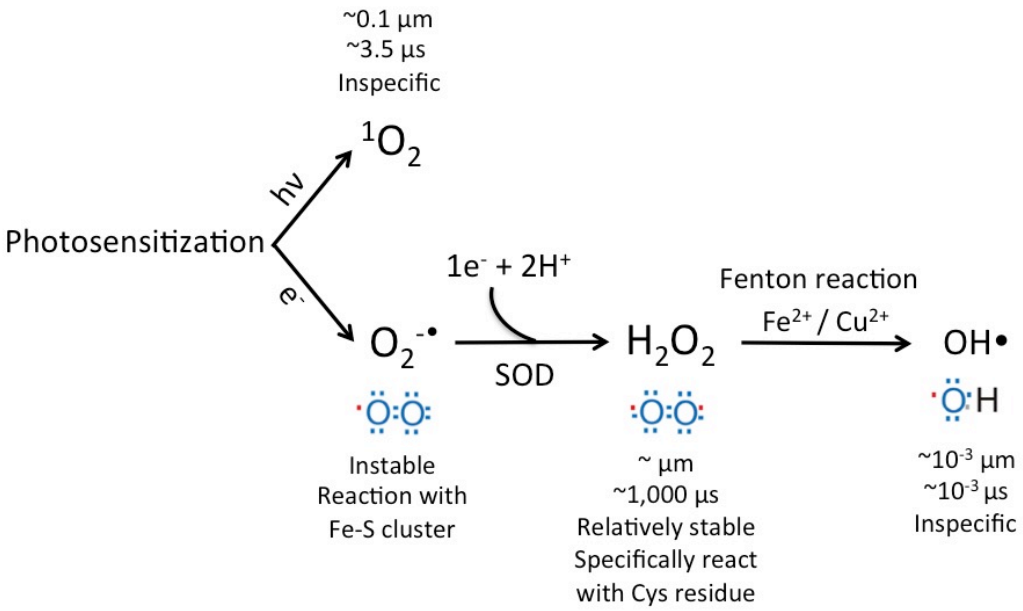

Figure 2.1. Different characteristics of ROS generated from photosensitization.

During cellular respiration that takes place in mitochondria, $O_2^{\bullet-}$ and its derivatives, H_2O_2 and $OH^{\bullet}$ are naturally formed upon incomplete reduction of oxygen. Roles of those species in maintaining physiological function in cell, in fact, have been widely well documented. $O_2^{\bullet-}$ is highly reactive toward Fe-S cluster and known to modulate transcription factor in *E. coli* via redox sensitive transcription factor SoxR (Winterbourn, 2008). H_2O_2 which specifically reacts to cysteine residue regulates gene transcription in *E. coli* via OxyR redox center. Since H_2O_2 is membrane permeable, it plays many roles in cellular events i.e. maintaining cellular redox potential, Ca^{2+} homeostasis, and apoptosis (Zorov et al., 2000). Changes in $O_2^{\bullet-}$ and its derivatives conncentration may control intracellular events (Schieber and Chandel, 2014). Unlike $O_2^{\bullet-}$ and its derivatives, $^1O_2$ are known to have unspecific target.

2.1.2 ROS of currently available genetically encoded photosensitizer

ROS type determination and its effectiveness to cause the damage are keys to characterize photosensitizers. For KillerRed, some experiments are done by changing the solution from H_2O to D_2O or scavenging experiments utilizing $O_2^{\bullet-}$ and its derivatives scavengers suggested that KillerRed actually produces $O_2^{\bullet-}$ rather than $^1O_2$. The electron transfer reaction may occur when chromophores are in excited state, resulting in the donation of an electron from the chromophore directly to $^3O_2$ or indirectly to other molecules near the chromophore that eventually react with $^3O_2$ to generate $O_2^{\bullet-}$. It was also suggested that the chain of water molecules inside the beta barrel may serve as electron wires, conducting electron transfer generated by excited chromophores to external molecules (Carpentier et al., 2009; Pletnev et al., 2009).

MiniSOG, on the other hand was identified as a generator of both $O_2^{\bullet-}$ and $^1O_2$. FMN undergoes photoinitiated electron-transfer reaction to produce $O_2^{\bullet-}$ and also energy transfer to ground-state oxygen to produce $^1O_2$ when irradiated with blue light (~440 nm) (Barnett et al., 2018; Pimenta et al., 2013; Shu et al., 2011). Generation of SOPP by reducing hydrogen bonding between FMN and its surrounding amino acid was aimed to suppress the photoinitiated electron transfer that producing $O_2^{\bullet-}$ which competes with $^1O_2$ production. Therefore, miniSOG improvements have been directed towards a complete $^1O_2$ generation (Westberg et al., 2015)

For those different properties among photosensitizers, it is necessary to choose the right photosensitizer for certain experiment. For example, to promote inactivation of cysteine rich protein target, photosensitizer that generates $O_2^{\bullet-}$ and H_2O_2 would be preferable over $^1O_2$ generator. Some factors to be considered are— 1) suitable type of

ROS for the purpose, 2) range of action, and 3) effectiveness of ROS generation by photosensitizer.

2.2 Purpose and significance

Photosensitizing capability of SNG was evaluated in bacterial and mammalian cells compared to other photosensitizing proteins. $^1O_2$ and $O_2^{\bullet -}$ measurements were done to assess type of ROS generated by SNG in order to predict in which condition SNG would be more useful for application rather than miniSOG and its improved variants.

2.3 Materials and methods

2.3.1 Phototoxicity in *E. coli* cells

To assess phototoxicity in *E. coli* cells, SNR/SNG/miniSOG/mCherry/EGFP-pRSET$_B$ were transformed into JM109(DE3) cells then cultured on LB plate (amphicillin selection) for 37°C overnight. Single colony was picked and cultured in 10 mL LB containing 0.1 mg/mL carbenicillin and shaked at 120 rpm for 72 hours. OD was measured at 600 nm and adjusted to 0.1. After OD was adjusted, 1 mL culture was centrifuged at 15,000 rpm and cell pellets were resuspended in PBS and kept on ice. 15 μL of suspension were subjected for light irradiation on Terasaki dish with 17.8 mW/cm^2 excitation light for 15 minutes from Xenon-arc lamp. Filters used for SNR/mCherry, SNG/miniSOG, and EGFP were 580AF20 (Omega), 447/60-25 (Brightline) and 475/42-25 (Brightline) respectively. After light irradiation, suspension were diluted at 10, 10^2, 10^3, 10^4, 10^5 and 10^6 dilution factor and cultured on LB plate using drop plate method. Colony forming unit was calculated as per log reduction of non-irradiated samples and irradiated samples.

2.3.2 Phototoxicity in mammalian cells

To assess SNG ability to induce cell death in mammalian cells, first, HeLa cells were plated on 35 mm glass bottom dish a day before transfection. On transfection day, HeLa cells were transfected with pcDNA3.1 plasmids encoding SNR, SNG, miniSOG, mCherry and EGFP using the calcium phosphate transfection method. Cell ablation experiment was performed 2 days after transfection, by irradiating cells on a fluorescence microscope (Nikon Eclipse TE2000-E, Oil immersion 60X Plan Apo objective lens, NA 1.4) for 2 mins with 2 W/cm^2 excitation light from Intensilight C-HGFIE (Nikon). Excitation filters used for this experiment were 447/60-25 (Brightline), 475/42-25 (Brightline) and 562/40 (Brightline) for SNG/miniSOG, EGFP, and SNR/mCherry respectively. DIC images were taken using an ORCA-FLASH 4.0 (Hamamatsu Photonics) every hour until 7 hour post-light irradiation.

2.3.3 Singlet oxygen ($^1O_2$) measurement

In vitro $^1O_2$ generation measurement was performed using ADPA (anthracene 9, 10-dipropionic acid) as $^1O_2$ sensor (Molecular probes). Mix of ADPA and protein were diluted in PBS to make final concentration 7.9 μM and 2 μM for ADPA and protein respectively). Solution was placed in cuvette then irradiated by 47 mW/cm^2 excitation light (438/24, 475/28, and 542/27 nm) from Light Engine Spectra (Lumencor) for 5 mins. Fluorescence intensity of ADPA (ex/em = 350/430 nm) was measured every 1 min during light irradiation using F7000 fluorescence spectrophotometer (Hitachi).

To assess $^1O_2$ generation in mammalian cells, HeLa cells transfected with pcDNA3.1 plasmids encoding sensitizer protein with mitochondria translocalization signal were incubated with 25 nM Si-DMA (Dojindo) in DMEM/F12 without phenol red

(ThermoFisher Scientific) for 45 mins at 37^{o}C. Cells then were irradiated with 4 W/cm^{2} 447/60-25 nm (Brightline) light from mercury arc lamp as light source for 10 s. Images were taken before and after irradiation at Cy5 channel (633 nm laser) with Nikon A1 confocal system (Nikon).

2.3.4 Superoxide ($O_2^{\bullet-}$) measurement

To assess $O_2^{\bullet-}$ generation, HeLa cells expressing SNG or miniSOG were incubated with 1-2 μM MitoSOX (ThermoFisher Scientific) in DMEM-F12 without phenol red for 10 mins. Cells were irradiated with excitation light similar to Si-DMA experiment for 30 s. Images were taken before and after light irradiation at RFP channel (with 543 nm excitation laser). ROI was made within cells using NIS Elements Software (Nikon) then fluorescence intensity was compared between before and after light irradiation.

To perform quenching experiments, HeLa cells expressing SNG and miniSOG plated on 96 well-plates were prepared a day before the experiment. One hour before irradiation, cells were treated with 200 U/mL PEG-SOD (Sigma Aldrich), 1000 U/mL catalase from bovine liver (Wako) or 60 mM mannitol (Wako) in DMEM-F12 without phenol red. After incubation at 37^{o}C for 1 hour, cells were washed with PBS three times then irradiated under fluorescence microscope (Nikon Eclipse TE2000, Oil immersion 40X Plan Apo objective lens, NA 1.4) with 2 W/cm^{2} 447/60-25 nm (Brightline) excitation light from Light Engine (Lumencor) for 2 mins. After light irradiation, DIC images were taken using ORCA-FLASH 4.0 Camera (Hamamatsu Photonics) every 1 hour for 6 hours post-light irradiation.

2.3.5 Statistical analysis

All data fitting and statistical analysis in this study were performed using Origin 8 software (OriginLab) and SPSS statistics (IBM). Statistical values including the exact N and statistical significance are reported in figure legends.

2.4 Results and discussion

2.4.1 SNG phototoxicity in *E. coli* cells as initial screening step

As initial screening of SNG photosensitization capability, SNG and other photosensitizer protein were expressed in *E. coli* then the colony forming unit/mL value between the irradiated and unirradiated cells were compared. As the result, irradiation of *E. coli* cells expressing SNG decreased the cell numbers similar to SNR. MiniSOG showed higher reduction of cell numbers than EGFP and SNR. Meanwhile, EGFP and mCherry, as negative control for 440 nm and 580 nm irradiation respectively, did not show decrease in cell number ($p<0.05$, student t-test) (Fig 2.2).

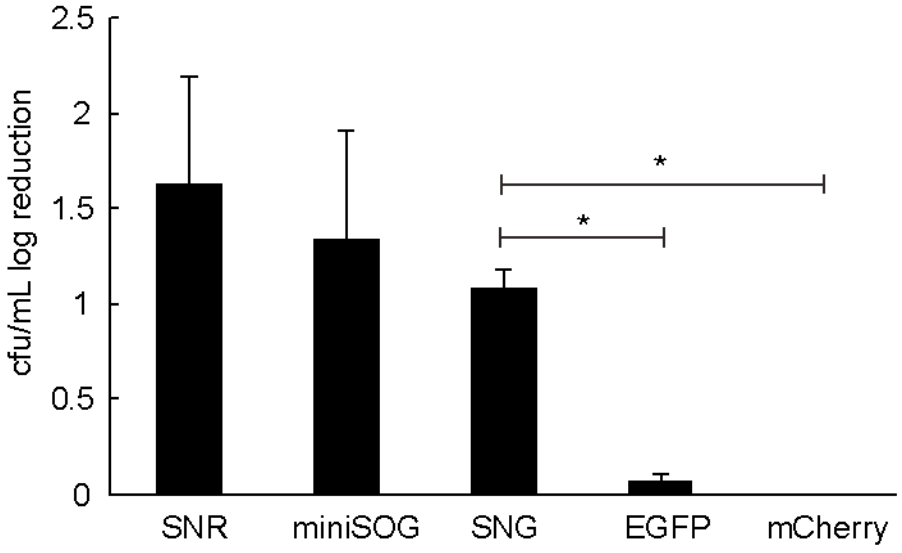

Figure 2.2. SNG and other photosensitizer protein phototoxicity in *E. coli* cells. EGFP and mCherry served as negative control for light irradiation.

2.4.2 Photo-induced mammalian cell ablation utilizing SuperNova Green

To assess SNG capability to generate ROS, SNG phototoxicity compared to other photosensitizing protein was assessed in *E. coli* and mammalian cells. I assessed the ability of SNG to induce cell death by irradiating HeLa cells expressing SNG targeted to mitochondria matrix. Upon increasing of ROS concentration, mitochondria would release cytochrome c to the cytosol then initiate cell signaling to induce cell death. As the result, after 2 W/cm^2 light irradiation for 2 mins, SNG caused cell death faster than SNR yet slower than miniSOG. As negative control for excitation light irradiation, EGFP and mCherry expressing HeLa cells irradiated with same condition as SNG and SNR, no significant cell death was observed indicating that irradiation by light itself does not cause cell death within this time frame (Figure 2.3). This result indicates that SNG has ROS generation ability to induce cell death.

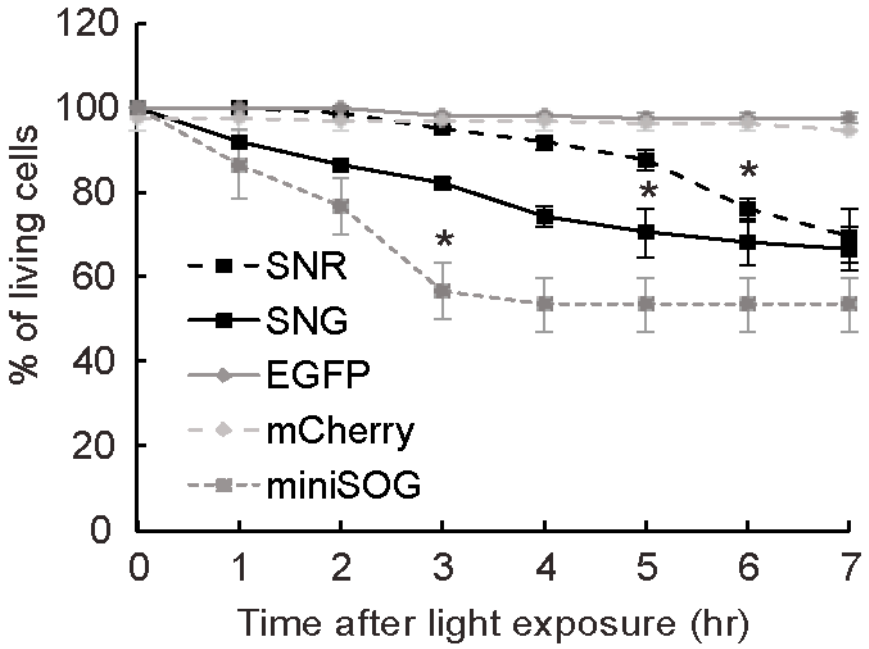

Figure 2.3. SNG phototoxicity in mammalian cells (a) Phototoxicity of SNG (■, black solid line) compared to SNR (■, black dashed line), miniSOG (■, grey dashed line), EGFP (◆, grey solid line) and mCherry (◆, light grey dashed line) targeted to matrix mitochondria in HeLa cells. Time dependent significant cell death (*) was analyzed for each hour post-irradiation to t_0. Significant cell death was found after 3

hours, 5 hours and 6 hours for miniSOG, SNG and SNR respectively ($p<0.05$, One-way ANOVA, Tukey, n = 144 cells for SNR, 128 cells for SNG, 73 cells for miniSOG. Cells were calculated from 8 images per construct). No significant cell death was observed for EGFP and mCherry expressing HeLa cells ($p>0.05$, One-way ANOVA, Tukey, n = 117 cells for EGFP, 149 cells for mCherry. Cells were calculated from 8 images per construct).

2.4.3 Photosensitization mechanism of SuperNova Green

2.4.3.1 Singlet oxygen measurement

To characterize which ROS does SNG produce, $^1O_2$ generation of SNG was measured in comparison to miniSOG upon irradiation of 438/24 nm light. Using previously known $^1O_2$ probe, anthracene 4,9 dipropionic acid (ADPA), generation of $^1O_2$ was assessed by measurement of ADPA fluorescence decay in time dependent manner which corresponds to the formation of endoperoxide adduct (Figure 2.4a) (Bresolí-Obach et al., 2016; Lindig et al., 1980). As the result, SNG did not cause significant ADPA fluorescence decay compared to miniSOG (Figure 2.4b), which is known to produce both $^1O_2$ and $O_2^{\bullet-}$ (Barnett et al., 2018; Pimenta et al., 2013; Ruiz-González et al., 2013; Shu et al., 2011). This result indicates that $^1O_2$ generated from SNG was much lower compared to miniSOG. When compared to KillerRed and SNR, which are known to mainly produce $O_2^{\bullet-}$ rather than $^1O_2$, and also EGFP and mCherry as negative control, SNG did not produce significant amount of $^1O_2$ (Figure 2.4c). ADPA alone did not bleach upon several excitation light irradiation (Figure 2.4d).

Previously, it was reported in (Ruiz-González et al., 2013) that ADPA may also respond to $O_2^{\bullet-}$ thus questioned the ADPA bleach of miniSOG in this experiment. Allegedly, amount of $O_2^{\bullet-}$ generated by KillerRed/SNG/SNR via such power density was not enough to significantly bleach ADPA as much as $^1O_2$ and/or $O_2^{\bullet-}$ generated by miniSOG.

To further assess SNG ability to produce $^1O_2$, I used Si-DMA (Silicone-containing rhodamine-9,10-dimethylanthracene), a far-red $^1O_2$ sensor which is specific to $^1O_2$ but not responsible to $O_2^{\bullet-}$, H_2O_2 or other ROS (Kim et al., 2014). Upon reaction with $^1O_2$, Si-DMA converts into bright form Si-DMEP ([7-(Dimethylamino)-9,9-dimethyl-10-(9,10-dimethyl-9,10-epidioxy-9,10-dihydroanthracene-2-yl)-9-sila-2,9-dihydroanthracene-2-ylidene]dimethyliminium). After comparing HeLa cells expressing SNG treated with Si-DMA before and after light irradiation, SNG does not produce significant amount of $^1O_2$ compared to normal HeLa cells while cells expressing miniSOG does (Figure 2.4e). Similar to ADPA experiment, $^1O_2$ measurement with Si-DMA indicated that unlike miniSOG, SNG does not produce $^1O_2$.

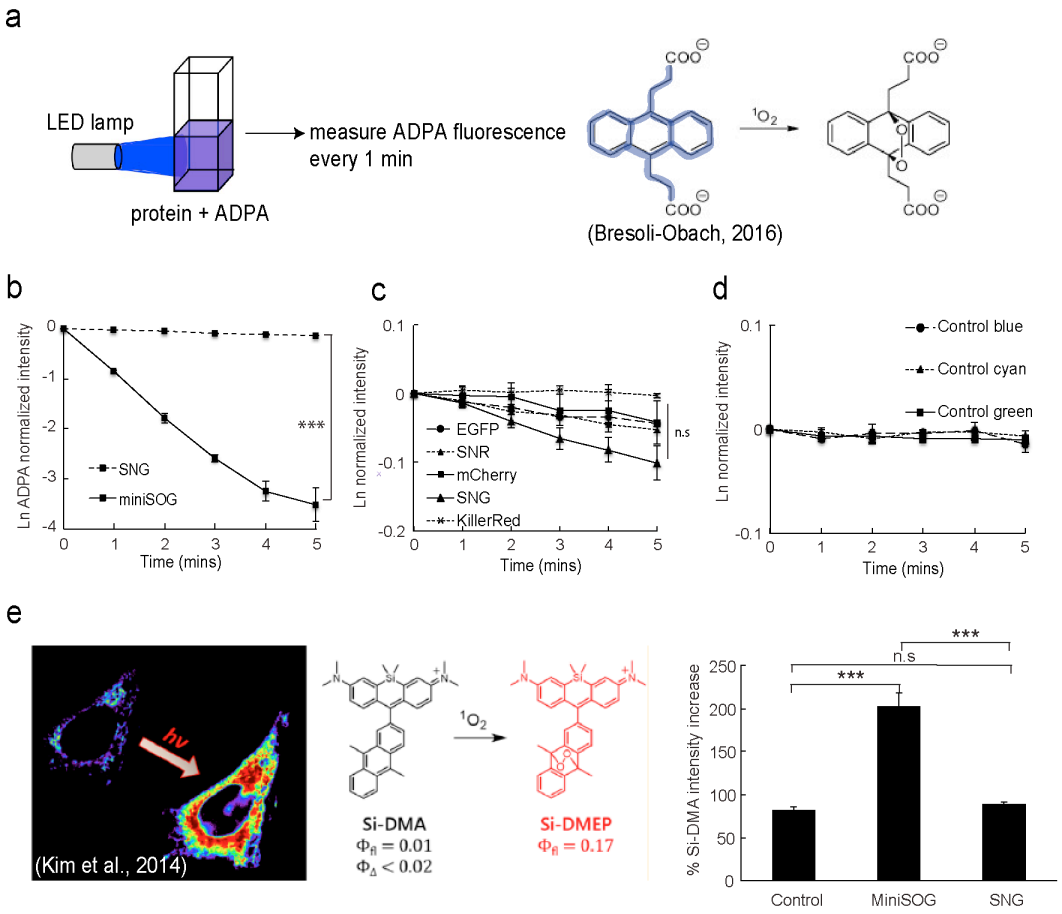

Figure 2.4. (a) Illustration of $^1O_2$ measurement using ADPA. Upon reaction with $^1O_2$, ADPA fluorescent will decay. (b) Time course of SNG and miniSOG $^1O_2$ measurement upon excitation light irradiation. Irradiation of miniSOG caused significant ADPA fluorescent decay compared to SNG ($p<0.001$, t-test, n = 4 replicates for miniSOG, 6 for SNG; each replicate came from independently purified protein samples). (c) ADPA fluorescence decay of SNG compared to KillerRed, SNR, EGFP and mCherry as a negative control. SNG did not cause significant ADPA bleaching ($p>0.05$, one-way ANOVA, n = 3 replicates for KillerRed, 4 for SNR, 4 for EGFP and 4 for mCherry, each replicate came from independently purified samples). (d) ADPA fluorescence upon light irradiation with 438/24 and 575/25 nm (n = 3 replicates for each control). No significant ADPA fluorescence decrease occurred. (e) $^1O_2$ measurement in HeLa cells expressing SNG or miniSOG in mitochondria matrix using Si-DMA. Upon reaction with $^1O_2$, Si-DMA will convert to Si-DMEP that emits red fluorescent. After 10 s light irradiation with 4 W/cm^2 excitation light, significant Si-DMA fluorescence intensity increase was observed for HeLa cells expressing miniSOG (compared to control, independent t-test, $p<0.001$, n = 100 cells) but no significant difference between SNG and control ($p = 0.185$).

2.4.3.2 Superoxide anion and its derivatives measurement

Since $^1O_2$ measurement result indicates that SNG does not work through energy transfer mechanism, I speculated that SNG produce other ROS that generated via electron transfer mechanism in keeping with its predescessor, SNR and KillerRed (Pletnev et al., 2009; Takemoto et al., 2013a; Vegh et al., 2011). To test this speculation, MitoSOX, a hydroethidine (HE) based redox probe that conjugated to triphenylphosphonium group (TPP^+) to target it to mitochondria was used. HE would react with $O_2^{\bullet-}$ to form 2-hydroxyethidium (2-OH-E^+). However, still there is no ideal $O_2^{\bullet-}$ sensor that allows vast and real time observation of $O_2^{\bullet-}$ only. HE is also known to react with other ROS (H_2O_2 and nitric oxide), peroxidase or redox-active metal ions (iron or copper) to form non-specific product ethidium (E^+) that together with 2-OH-E^+ emits red fluorescence. However, it was shown previously that HE did not react with $^1O_2$ (Barnett et al., 2018) which become advantageous for this study since our purpose is to differentiate $^1O_2$ or $O_2^{\bullet-}$ and its derivatives formation.

As the result, ROS generation in HeLa expressing miniSOG or SNG in matrix mitochondria shows significant red fuorescent increase of MitoSOX compared to control and yet no significant difference was found between miniSOG and SNG (Figure 2.5a). Here, I conclude SNG and miniSOG produce same amount of ROS other than $^1O_2$ when applied in mammalian cell.

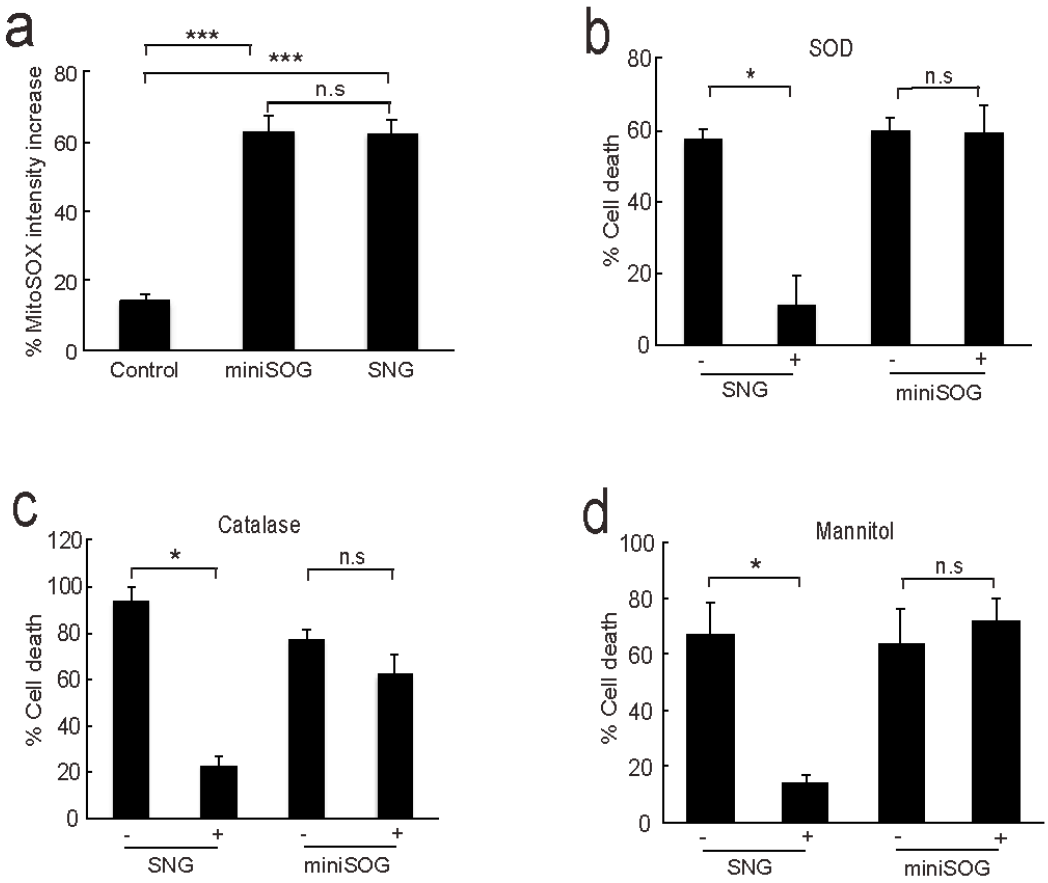

Figure 2.5. (a) MitoSOX fluorescence intensity increase in cells expressing miniSOG and SNG. Compared to control, miniSOG and SNG showed significant increase (independent t-test, $p<0.001$, n = 100 cells) but no significant difference between SNG and miniSOG fluorescence change ($p = 0.659$). (b), (c) and (d) showed $O_2^{\bullet-}$, H_2O_2 and $OH^{\bullet}$ quenching experiment using 200 U/mL SOD, 1000 U/mL catalase and 60 mM mannitol respectively applied to HeLa cells expressing mitochondria matrix localized miniSOG and SNG. HeLa cells expressing SNG treated (+) with SOD (b), catalase (c) and mannitol (d) showed significant reduction in cell death after light irradiation when compared to non-treated (-) cells ($p<0.05$, t-test, n = 45 cells for SNG (-) SOD, 38 cells for SNG (+) SOD; 40 cells for SNG (-) catalase, 94 cells for SNG (+) catalase; n = 220 cells for SNG (-) mannitol, n = 185 cells for SNG (+) mannitol; images were calculated from 4 images for each condition. HeLa cells expressing miniSOG showed no reduction in cell death ($p>0.05$, t- test, n = 59 cells for miniSOG (-) SOD, 62 cells for miniSOG (+) SOD; 67 cells for miniSOG (-) catalase, 93 for miniSOG (+) catalase; n = 155 cells for miniSOG (-) mannitol, 180 cells for miniSOG (+) mannitol cells; images were calculated from 4 images for each condition). Error bar represents ±SEM.

There are other methods to predict production of ROS without fluorescent ROS sensors. A conventional yet widely used method is to quench the ROS with scavenging molecules. By comparing the effect between the non-treated samples and

treated samples with scavenging molecules, ROS presence / effect could be detected. Although could only measure ROS production qualitatively and indirectly, this method could specifically detect which type of ROS presents in the sample since several available commercial molecules are specific to certain type of ROS. Here I used 200 U/mL SOD, 1000 U/mL catalase and 60 mM mannitol to specifically scavange $O_2^{\bullet-}$, H_2O_2 and •OH respectively. Concentration of each scavanging molecules is determined following previous studies (He et al., 2016; Makhijani et al., 2017). To assess the presence of those types of ROS as product from photosensitizing, cells were irradiated with excitation light as previously described in 2.3.3. After light irradiation, cell death was observed for 7 hr post-irradiation and number of cell death was compared between the treated and non-treated cells with scavenging molecules.

As the result, there was significant decrease of cell death observed from cells expressing SNG treated with SOD, catalase and mannitol but not from cells expressing miniSOG (Figure 2.5b,c,d). Since miniSOG produces both $^1O_2$ and $O_2^{\bullet-}$, theoretically, expected result of miniSOG scavenging experiment is a slight decrease in cell death. However, based on our result, ROS generated by miniSOG could not be scavanged by SOD, catalase or mannitol. During the experiment, I observed apparent bleaching of miniSOG due to light irradiation (2 W/cm^2 light irradiation for 2 mins) (data not shown). As previously reported, photobleaching is correlated with increase of miniSOG $^1O_2$ generation. Therefore, I speculated that SOD, catalase and mannitol could not limit the ability of miniSOG to cause cell death due to dominant $^1O_2$ over $O_2^{\bullet-}$ generation by miniSOG in this particular experiment.

Based on these experiments, I made some speculations about SNG mechanism to produce ROS as photosensitizer. $O_2^{\bullet-}$ as the primary ROS produced from excited chromophore will undergo dismutation to H_2O_2 then fenton reaction to •OH. The treatment with those scavangers above has reduced the effect of ROS that may lead to cell death. However, since scavenging $O_2^{\bullet-}$ and H_2O_2 does not produce a total non-reactive species, mechanism of which SOD and catalase could safe the cells from cell death remains a question. A more quantitative and specific measurement of each ROS species produced by SNG using a more specific sensor would help to reveal those mechanisms.

2.4.3.3 Discussion

Here I showed that our green monomeric photosensitizer has different characteristics compared to other available green variant of photosensitizer, such as miniSOG and its improved variants. As previously mentioned, miniSOG ability to generate ROS depends on the concentration of FMN, its chromophore. Thus, in the condition where the FMN cofactor is absent or scarce, miniSOG phototoxicity would be ineffective (Ryumina et al., 2013). Moreover, unlike SNG, which produces $O_2^{\bullet-}$ (and its derivatives), original miniSOG produces both $O_2^{\bullet-}$ and $^1O_2$ (Barnett et al., 2018; Pimenta et al., 2013; Ruiz-González et al., 2013). Other currently available successors of miniSOG: SOPP (Westberg et al., 2015), SOPP2 and SOPP3 (Westberg et al., 2017) were directed towards complete $^1O_2$ generation which makes them different than SNG.

Not only $O_2^{\bullet-}$ and its derivatives are normally produce in normal cell physiology, they also have essential role in controlling intracellular events (Schieber and Chandel,

2014). Therefore, not only protein inactivation or cellular ablation, SNG would be useful to manipulate cell behaviour or elucidate subcellular ROS function in intracellular events.

2.5 Summary

ROS measurement using fluorescent ROS sensor and scavenging molecules has shown that SNG produces undetectable amount of $^1O_2$ yet more specific to other ROS that are produced through electron transfer mechanism.

CHAPTER 3: SELECTIVE PROTEIN INACTIVATION AND CELL ABLATION

3.1 Introduction

3.1.1.1 Multi-CALI

There are abundant and unaccountable numbers of protein that interact direct/indirectly to control cellular functions. Sometimes inactivation of those proteins at the same time gives distinct result with separated temporal inactivation. Moreover, deactivating two different kinds of protein within single cell in subcellular precision would give different result than deactivating the whole protein populations present in the cell. Inactivating different kinds of protein within subcellular region and miliseconds time scale could only be realized using different colour variants of photosensitizer.

3.1.1.2 Multi-cell ablation

As briefly mentioned in 1.1.1.3, similar as chemical dye based photosensitizers, genetically encoded photosensitizer is useful to induce cell death. Targeting cancer cells using an anti-receptor antibody-KillerRed/miniSOG fusion protein as a genetically encoded immunophotosensitizer has demonstrated fine targeting properties and efficiently killed p185 (HER-2-ECD)-expressing cancer cells upon light irradiation *in vitro* (Mironova et al., 2013; Serebrovskaya et al., 2009). Other methods include targeting to the inner and outer membrane of mitochondria, nucleus, plasma membrane, lysosome, and peroxisome have been attempted and shown to

achieve cell ablation *in vitro* and *in vivo* experiments (Liao et al., 2014; Ryumina et al., 2013, 2016; Serebrovskaya et al., 2013; Shirmanova et al., 2015, 2013a)

Based on those targeting efforts to approach cellular ablation with photosensitizer, scaling up photosensitizer application from cellular to organism is now become practical. For example, application of mitochondria targeted KillerRed *in vivo* has been done to kill cardiomyocytes cells in zebrafish to make inducible heart-failure animal models (Buckley et al., 2017; Teh and Korzh, 2014). KillerRed was also demonstrated in *C. elegans* to induce cell ablation of AWA sensory neurons, allowing manipulation of *C. elegans* chemotaxis behaviour toward AWA sensitive attractants. These experiments showed that inducing cell ablation *in vivo* would allow *in situ* study of animal development and behaviour (Kobayashi et al., 2013).

Similar as protein interaction complexity in single cell, cells are also communicated with each other to synergistically or antagonistically modulate function in a tissue, organ or organism. Over decades, people have been trying to answer the questions of complex neural circuit which is still become a major focus in neurobiology. For instance, how signals were transmitted in certain behaviour and how one signal may result in several possible responses. To solve this problem, one of the approaches is to ablate certain cell inside the complex circuit then see the effect to the behaviour. Similar case to protein inactivation, ablation of two or more diffferent kind of cells in an independent spatiotemporal manner could be done using different colour of photosensitizers. In this study, I will prove that selective cell ablation using combination of SNG and SNR is approachable.

3.2 Purpose and significance

The purpose of this experiment is to test if ROS generation by SNG could induce CALI in a subcellular range when specifically induced by blue light illumination but not other wavelengths. Then, as a proof of concept for multi-CALI purpose, SNG-SNR combination was used to independently inactivate protein when irradiated with blue or orange light in regard to SNG and SNR excitation light respectively. To our knowledge, this experiment is the first demonstration of selective CALI utilizing two colours of photosensitizer performed within single cell.

Scaling up the application from subcellular region to cellular level, selective cell ablation of cancer cells was performed by targeting SNG and SNR to matrix mitochondria. This demonstration would serve as proof of concept for application of multi-spatiotemporal cell ablation in organism.

3.3 Materials and methods

3.3.1 Gene construction

For selective CALI experiment, SNG and SNR were used to inactivate Pleckstrin Homology domain (PH domain) of Phospholipase C delta-1 (PLC-δ_1). PH domain sequence was obtained from GFP-C1-PLCdelta-PH (Addgene #21179). Further, fusion proteins of PH domain tagged with photosensitizer and fluorescence reporter were generated using restriction sites as follow: *Age*I-Venus-*Bgl*II-PH-*Xba*I-SNG-*Eco*RI and *Age*I-mNeptune-*Bgl*II-PH-*Xba*I-SNR-*Eco*RI. All fragments were generated with KOD Plus PCR mix (Toyobo) then restricted with respective restriction enzyme. Digested fragments were cloned to C1 plasmid disgested with

*Age*I and *Eco*RI. All oligonucleotides using to amplify cDNA fragments are all listed in Supplementary data: Table S1.

3.3.2 Selective CALI

One day before transfection, HEK 293T cells were plated on 35 mm glass bottom dish to reach 70% confluency the next day. HEK293T cells were co-transfected using Lipofectamine 2000 with Venus-PH-SNG/C1 and mNeptune-PH-SNR/C1. Selective CALI experiment was performed 48 hours post-transfection with confocal microscope (A1 Nikon Confocal, Nikon Eclipse Ti). HEK293T cells were subjected to light irradiation using Intensilight (Nikon) with ~3W/cm^2 447/60-25 and 562/40 nm in respect to SNG and SNR excitation light under 60x oil immersion objective lens NA 1.4 (Nikon) for 10 s. Images of Venus and mNeptune fluorescence were taken using 488 nm laser and 633 nm laser at time 0 (before light irradiation), 10 s (immediately after light irradiation), 1 min, 5 mins, and 15 mins. To analyze the effect of CALI to distribution of Venus and mNeptune fluorescence inside cells, fluorescence intensity of cytoplasm and plasma membrane of cells were measured using QuimP plugin (Dormann et al., 2002) in Fiji Software (Schneider et al., 2012). Increase of cytoplasm and plasma membrane fluorescence intensity in a time dependent manner was calculated as:

$$\Delta\text{Ratio} = \frac{\text{Icytoplasm}\,t_x}{\text{Imembrane}\,t_x} - \frac{\text{Icytoplasm}\,t_0}{\text{Imembrane}\,t_0}$$

t_x means timepoint after light irradiation and t_0 means timepoint before light irradiation.

3.3.3 Selective cell ablation

To perform selective cell ablation, first, stable cell lines expressing SNR or SNG translocalized to mitochondria matrix were generated by transfection of COXVIII2x-SNR/SNG-pcDNA3.1 to HeLa cells using Lipofectamine 2000. Antibiotic selection was done using 400 μg/mL geneticin (Invitrogen). Cells expressing SNR and SNG were then co-cultured on 30 mm glass bottom dishes a day before selective cell ablation experiment. Cells were subjected to ~4W/cm^2 447/60-25 nm and 562/40 nm light irradiation (mercury arc lamp) for 2 mins to ablate SNG and SNR expressing cells respectively. To observe cell death, DIC images were taken at 0, 3, 5 hr post irradiation with Nikon Eclipse TE2000-E (Nikon, Oil immersion 60X Plan Apo objective lens, NA 1.4) equipped with ORCA-FLASH 4.0 (Hamamatsu Photonics). Cell deaths were determined by apoptosis or necrosis like morphology (apparent shrinking or blebbing). Percentage of cell death was compared between SNG and SNR expressing cells in both 440 nm and 560 nm light irradiation.

3.4 Results and discussion

3.4.1 Selective CALI

To proof SNG ability to initiate CALI and to test its compatibility when concomitantly used with SNR, SNG and SNR were targeted to pleckstrin homology domain (PH domain) of phospholipase C delta-1 (PLC-δ_1) that binds to inositol 1,4,5-tris-phosphate (Ins[1,4,5]P_3) at the plasma membrane (Várnai and Balla, 1998). The expected result was that selective photosensitizer mediated ROS generation by blue or orange light would cause PH domain detachment from PLC-δ_1. To monitor this effect, N-terminal of PH domain was tagged with fluorescent probe that would be liberated

together with PH domain into the cytosol upon CALI. For that purpose, mNeptune2.5-PH-SNR and Venus-PH-SNG were constructed as fluorescent probe - protein target - photosensitizer fusions. Monitoring fluorescence distribution of mNeptune2.5 and Venus in plasma membrane and cytosol would allow visualization of PH domain before and after its inactivation caused by the responsible photosensitizer, SNR or SNG (Figure 3.1a). EGFP-PH-KillerRed and EGFP-PH were used as positive and negative controls respectively.

Images of HEK293T cells expressing EGFP-PH show localization of EGFP to plasma membrane at time 0. After irradiation with 3 W/cm^2 of 440 nm light for 10 s, cells expressing the EGFP-PH did not show cytoplasm/membrane intensity ratio change. This result suggests that 440 nm light irradiation itself did not cause PH domain inactivation. Following previous study by Bulina and colleagues (2013), EGFP-PH-KillerRed was used as positive control. As expected, cells expressing EGFP-PH-KillerRed showed an increase in cytoplasm/membrane intensity ratio after 560 nm light irradiation (Figure 3.1b, left panel; 3.1c,i) meaning that 3 W/cm^2 of light irradiation is enough to cause PH domain inactivation.

For the selective CALI experiment, HEK293T cells co-expressing mNeptune-PH-SNR and Venus-PH-SNG were irradiated with 3 W/cm^2 of 560 nm light for 10 s to inactivate PH domain by SNR. By comparing images taken in the Venus and mNeptune channel, after light irradiation, there was a significant increase of mNeptune ratio but not Venus ratio (Figure 3.1b, center panel; 3.1c, ii) meaning that 560 nm light irradiation could only activate SNR but not SNG. On the other hand, when co-transfected cells were with 3 W/cm^2 440 nm light to inactivate PH domain

by SNG, the opposite result was observed. There was no significant increase of mNeptune ratio but significant increase of Venus ratio. The slight increase of mNeptune ratio observed after 440 nm light irradiation (Figure 3.1b, right panel; 3.1c, iii) might due to the small absorbance peak of SNR at 440 nm (Figure 1.6c) thus, possibly small insignificant amount of SNR were also affected by this light irradiation.

It was feared that the light irradiation to take the images itself might activate the sensitizers. Therefore, light control experiments were done on cells expressing both Venus-PH-SNG and mNeptune-PH-SNR. Images of those cells were taken with similar laser power density as selective CALI experiment but without 3 W/cm^2 for 10 s light irradiation. Result showed that imaging using 488 nm and 633 nm laser did not cause significant effect to the sensitizers (Figure 3.1c,iv).

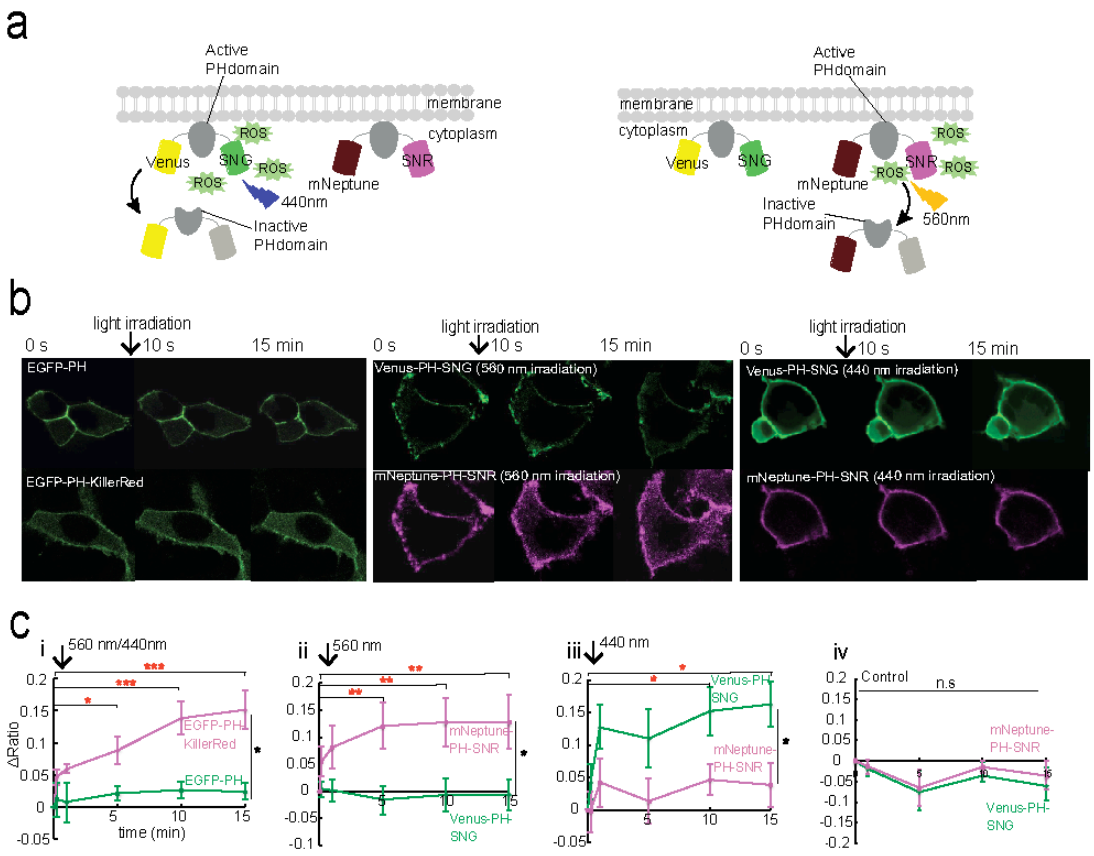

Figure 3.1. (a) Schematic overview of selective CALI in this experiment using SNG incombination with SNR activated with distinct excitation light to induce ROS production, which then results in detachment of inactive PH domain from plasma membrane. (b) Images of HEK293T cells expressing all constructs assesed in this experiment taken at 0 s (before ROS producing light irradiation), 10 s (immediately after light irradiation) and 15 min after 3 W/cm^2 light irradiation for 10 s. All constructs were localized to the plasma membrane prior to light irradiation. Fluorescence signal increased in cytoplasm after inactivation of the PH domain for EGFP-PH-KillerRed (560 nm irradiation), mNeptune-PH-SNR (560 nm irradiation) and Venus-PH-SNG (440 nm irradiation). (c) Quantitative measurement of fluorescence ratio increase between cytoplasm to plasma membrane normalized to R_0 (cytoplasm/membrane fluorescence ratio at t_0). (i) EGFP-PH-KillerRed showed significant ratio increase after 560 nm light irradiation ($p<0.05$, one-way ANOVA, Tukey, n = 10 cells). On the contrary, EGFP-PH domain as negative control did not show any significant changes. (ii) 560 nm light irradiation of Venus-PH-SNG and mNeptune-PH-SNR expressing cells caused a significant ratio increase of mNeptune fluorescence in a time dependent manner ($p<0.05$, one-way ANOVA, Tukey, n = 11 cells). R_{15} value of mNeptune was significally different when compared to Venus R_{15} ($p<0.05$, t-test, n = 11 cells for each construct). On the contrary, 440 nm light irradiation (iii) caused significant ratio increase of Venus fluorescence ($p<0.05$, one-way ANOVA, Tukey, n = 10 cells) as well as its R_{15} to mNeptune R_{15} ($p<0.05$, t-test, n = 10 cells for each construct). (iv) R value measurement of cells expressing Venus-PH-SNG and mNeptune-PH-SNR without light irradiation. No significant ratio changes over time. Error bar represents ±SEM.

This selective application of CALI utilizing SNG and SNR suggests that the technique can be performed without significant collateral damage to the non-target protein even when they are both in the same subcellular range, in this case, the plasma membrane.

3.4.2 Selective cell ablation

Selective cell ablation was performed on co-culture of HeLa cells expressing SNG and SNR to assess whether blue light irradiation could induce HeLa cells expressing SNG cell death while preserving viability of SNR expressing cells. Experiment was done by irradiation a field of view consisted of cells expressing SNR and SNG with 4 W/cm^2 of 440 nm light for 2 minutes. As the result, 94% of cells expressing SNG were successfully ablated while almost 100% SNR expressing cells survived (Figure 3.2.a). On the contrary, when the co-culture was irradiated with 560 nm at 4 W/cm^2 for 2 minutes, only cells expressing SNR were ablated while cells expressing SNG survived (Figure 3.2.b). In conclusion, similar as selective CALI, SNG in combination with SNR could incude specifically induce cell ablation with blue and orange light irradiation respectively.

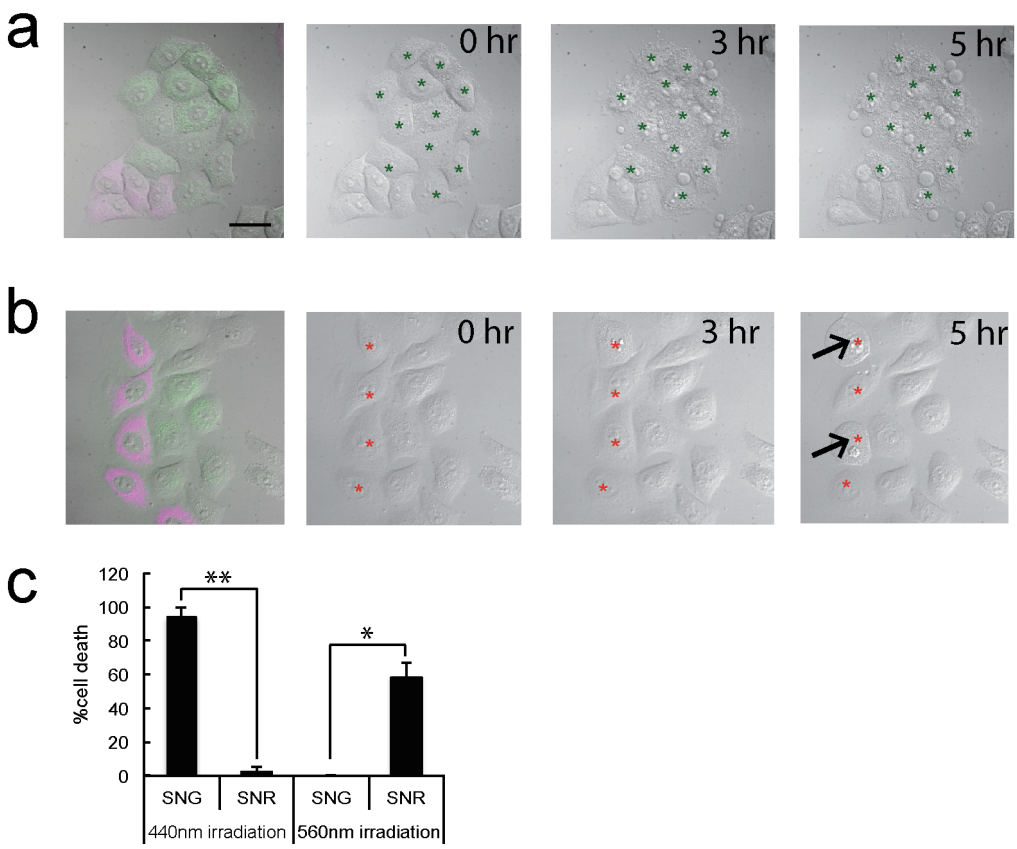

Figure 3.2. Selective cell ablation of co-cultures of HeLa cells stably expressing SNR and SNG in mitochondria. (a) Images of co-cultures irradiated with ~4 W/cm^2 blue light for 2 mins at 0, 3 and 5 hour post-irradiation. Cells expressing SNG underwent cell death while cells expressing SNR survived. (b) Images of co-cultures irradiated with ~4 W/cm^2 orange light for 2 mins and taken same as (a). Half of cells expressing SNR underwent cell death while all cells expressing SNG survived after 5 hour post-irradiation. (c) Quantitative analysis for selective cell ablation with 440 nm and 560 nm light irradiation. Under 440 nm light irradiation, significant cell death occurred for cells expressing SNG compared to SNR ($p<0.01$, t-test, n=97 cells). On the other hand, under 560 nm light irradiation, significant cell death occurred for cells expressing SNR compared to SNG ($p<0.05$, t-test, n=36 cells). Scale bar = 20 μm. Error bar represents ±SEM.

Apart from that, apparently SNG efficiency to ablate cell was higher than SNR as observed in Figure 3.2c and Figure 2.3. Approach to achieve similar killing efficiency by SNR has been done by increasing orange light power density. However, instead of increase killing efficiency by SNR, it caused unspecific cell killing of SNG expressing cell as well due to light toxicity (data not shown). In the future, there is a

room for improvement of SNR killing efficiency in order to achieve same efficiency with SNG.

3.4.3 General discussion

Since establishment of fluorescent sensor and advancement in imaging technique, current demand is to be able to catch moments of fast and dynamic biological phenomena. To visualize such phenomena, plenty of biological sensors have been made (e.g. Ca^{2+}, voltage, cell cycle indicator). When combination of fluorescence imaging and photosensitizer is needed to allow cause and effect to be visualized simultaneously, utilizing shorter excitation wavelength photosensitizer would be more preferred. The basic reason is that usually real-time imaging of a biological process or phenomena requires longer period of imaging while photosensitizing/inactivation process requires shorter time. Exposing living cells to short excitation wavelength (e.g UV or blue light) causes phototoxicity in cells itself. Thus, photosensitizing is better to be achieved at shorter excitation wavelengths, and visualize the effect at longer excitation wavelengths (Laissue et al., 2017). In this case, SNG has advantageous over other KillerRed based variants.

Some optogenetic tools have been used to manipulate cell behaviour and inactivate protein function. For instance by anchor-away method, target protein were photo-induced to localized far away from its target / functional region in cell (Valon et al., 2017) or photoinduced oligomerization by CRY2 (cryptochrome 2) / CIB1 (cryptochrome-interacting basic-helix-loop-helix) protein (Lee et al., 2014). However, those systems required complex construction of protein target and inhibitor/translocalization signal to CRY2/CIB1 component independently. Compared

to those systems, inactivation by SNG is more straightforward and only requires fusion to a specific protein. In addition to that, SNG causes irreversible inactivation thus when longer-term loss of function is favored, SNG has the advantages over the reversible CRY2/CIB1. But one must note that this longer-term loss of function by SNG would only work where the dissociation rates are faster than the protein turnover rate.

3.5 Summary

SNG has shown its ability to perform CALI of PH domain from PLC-δ_1 using the same experimental set up as reported CALI experiment with KillerRed. This study showed that green-red combination as widely used for multi-colour imaging (e.g EGFP-mCherry) is also useful for multi-colour CALI or cell ablation using SNG-SNR combination. Therefore, controlling multiple protein inactivation or cell ablation for function elucidation or behaviour manipulation of cell or organism will be possible to be achieved in a specific spatial and temporal manner.

CHAPTER 4: CONCLUDING REMARKS

4.1 Conclusion

Development of practical and specific photosensitizing tools to effectively inactivate protein/cell of interest has been keeping up with the research trend and needs. To enable multi-protein/cell inactivation in spatiotemporal manner as another advancement in CALI method, I established SNG, a monomeric green variant of genetically encoded photosensitizer to overcome the drawback of FMN dependency of miniSOG.

SNG was successfully established from monomeric variant of KillerRed, SNR, by introducing mutation to its chromophore and other position to prevent maturation of the chromophore to longer emission wavelength. Characterization of SNG as fluorescent protein has shown that SNG is excited by blue light (~440 nm) to emit green (~510 nm) emission. SNG faster photobleaching than EGFP might correlate to its ROS generation property. Moreover, SNG is an ideal genetically encoded photosensitizer for fusion protein or subcellular tag due to its monomeric property. *In vitro* and *in vivo* assessment of SNG monomericity has shown that SNG maintain its monomeric property at 10 uM protein concentration and when tagged to target protein or subcellular localization respectively.

ROS generation evaluation of SNG has shown that SNG dominantly generates ROS through electron transfer over energy transfer mechanism thus makes SNG produces $O_2^{\bullet-}$. Since $O_2^{\bullet-}$ is naturally produced in living cells and underwent dismutation and fenton reaction to produce H_2O_2 and •OH respectively, manipulation of this ROS

concentration intracellularly would as well help us to understand ROS role in cellular signaling/phenomena. In that case, SNG may be a better choice over miniSOG and its iterations, which produce $^1O_2$ species.

Apart from type of ROS that SNG produces, SNG has been shown in this study to specifically inactivate protein function as demonstrated to inactivate PH domain of PLC- δ_1. SNG is able to induce cell death as well when translocalized to matrix mitochondria. As a proof of concept of the advantages to have several colour variants of genetically encoded photosensitizer, SNG in combination with SNR is able to perform selective protein inactivation and cell ablation with blue and orange light irradiation respectively. In conclusion, establishment of SNG as a green monomeric photosensitizing fluorescent protein has brought new insight and new advancement to the optogenetic toolbox.

4.2 Perspectives

4.2.1 Simultaneous photo-induced protein inactivation and super-resolution imaging

Since its establishment over decades ago, inactivation of protein by ROS has been improved to meet relevant needs. In its early years, photosensitizer was mostly used in developmental biology and cancer mechanism. In 2000s, photosensitizers are applied to some time specific events in single cells. More than that, photosensitizers also have shown its handiness in manipulating animal behaviour.

Currently, all advancement in imaging technique always related to improve the speed or resolution of the image. The reason is because people are trying to catch moments of fast and dynamic biological phenomena. For instance, to image cell migration, people are focusing of turnover and dynamic changes of cytoskeletal and motor proteins. To observe this kind of phenomena, indeed a real-time imaging and good spatial resolutions are needed. Super-resolution is an imaging technique to visualize cell structure with resolution below diffraction limit.

After development of genetically encoded photosensitizer, nanoscale approach of protein inactivation becomes possible thus makes CALI method relevant to keep up with super-resolution imaging. The presence of SNG and other colour variants together with established super-resolution technique would help to reveal protein function in a vastly moving environment and enable visualization of the effect in a nanoscale range (Hell, 2003).

Furthermore, individual function of a molecule is often disregarded over population function. For example, DNA polymerase III is known to replicate *E. coli* genome but sometimes it is forgotten that only 10-20 molecules of DNA polymerase III holoenzyme are present per *E. coli* cell (Wu et al., 1984). How *E. coli* controls the distribution of these molecules is not yet well evaluated. Inactivation one molecule of those would enable assessment of what one single molecule can do to the *E. coli* replication process. Utilizing STED (Stimulated Emission Depletion Microscopy) (Hell and Wichmann, 1994) to illuminate single molecule of photosensitizer could lead to super-localized protein inactivation. This approach would be useful to target one single molecule of interest then to visualize the effect up to whole organism.

4.2.2 Potential triple photo-inducible protein inactivation and cell ablation

Establishment of SNG has expanded KillerRed based photosensitizer colour palette. The three colour variants of monomeric KillerRed, which are SuperNova Red, mKillerOrange and SuperNova Green, could be useful to spatiotemporally inactivate/ablate three different types of protein/cell in spatiotemporal manner. Previously it was shown that 510 nm light irradiation could only induce mKillerOrange but not KillerRed ROS generation. As a proof, here is shown that applying 510 nm light irradiation to cells expressing SNG in matrix mitochondria did not cause any significant effect. As expected, 510 nm light irradiation killed cells expressing mKillerOrange (Figure 4.1). This result indicates that three colour variants of genetically encoded photosensitizers may be possible to use in combination.

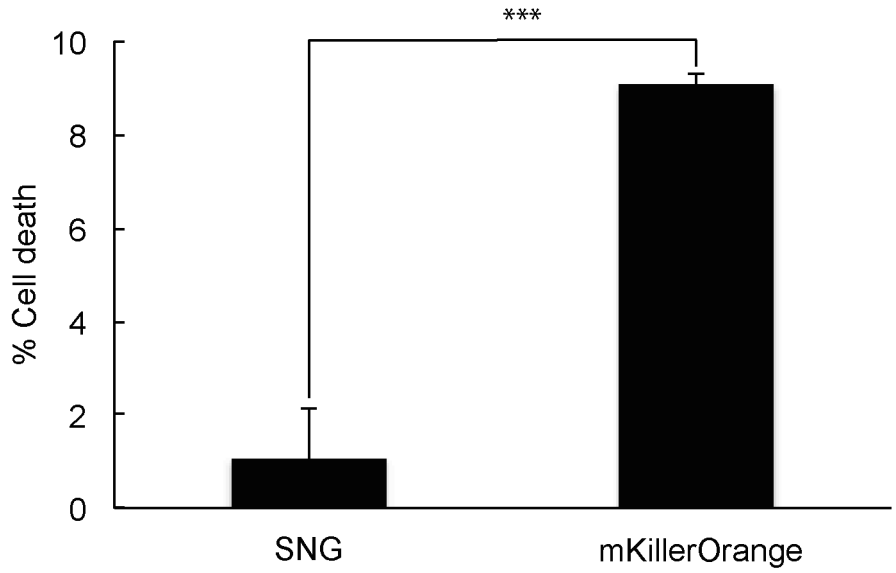

Figure 4.1. Selectivity between SNG and mKillerOrange upon 510 nm light irradiation. SNG and mKillerOrange phototoxicity in HeLa cells after light irradiation with ~1W/cm^2 510 nm for 2 mins (t-test, $p<0.01$, n = 141 cells for SNG, 89 cells for mKillerOrange. Cells were counted from 4 images for SNG and 3 images for mKillerOrange).

4.2.3 Bioluminescent based photosensitizer

Since inactivation of cell/protein within a functional organism would be useful for *in situ* loss of function observation *in vivo*, a demand for a tool that can perform this task is high. Altough utilizing currently available photosensitizer could achieve specific inactivation within an organism, long term light irradiation still become problematic since there are several endogenous chromophore that are also effective photosensitizers such as flavin mononucleotide and riboflavin (Bäumler et al., 2012; Pimenta et al., 2013). Ideally, in this situation, a light-free induced system would be preferable since it eliminates the unspecific phototoxic coming from excitation light and enable deep-tissue penetration.

Currently, chemiluminescent protein that emits light through reaction with substrate has shown advantages to overcome those drawbacks. When combined with bright fluorescent protein as BRET (Bioluminescent Resonance Energy Transfer) pairs, these tools have been shown to be able to visualize biological phenomena *in vitro* and *in vivo* without excitation light (Saito et al., 2012; Suzuki et al., 2016). Since one of the criteria to make a good BRET pair is absorption spectral overlap between donor (luminescent protein) and acceptor (fluorescent protein), in this case SNG would be an ideal pair for the brightest chemiluminescent protein to date, NanoLuc. Huge spectral overlap between SNG and NanoLuc would be possible for us to make the first bioluminescent photosensitizer for deep tissue targeting protein/cell inactivation.

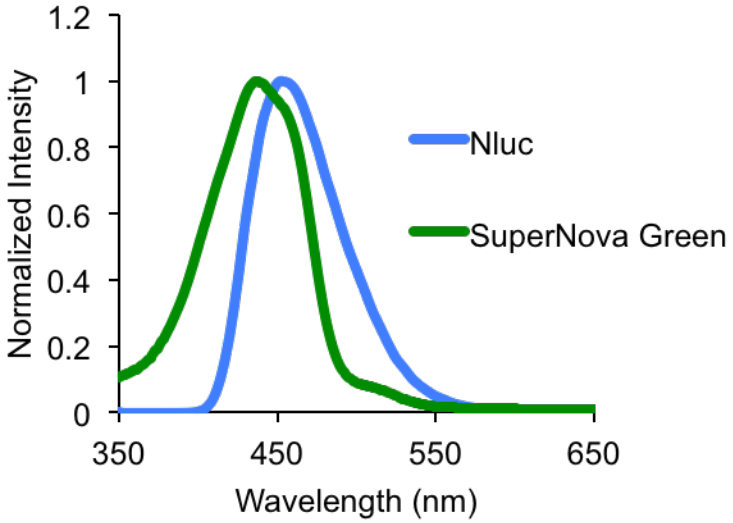

Figure 4.2. Spectral overlap between NanoLuc (Nluc) and SNG

ACKNOWLEDGEMENTS

This study was carried out from 2015 to 2018 at the Department of Biotechnology, Graduate School of Engineering, Osaka University.

First, I would like to express my deepest gratitute to my supervisor Prof. Takeharu Nagai for providing me a chance to pursue my PhD in Japan. Not only providing me many chances to connect with many professional scientists but also his trust in me that encourage me to always do my best.

I am very grateful to Associate Prof. Tomoki Matsuda who has supervised me since I joined Nagai Laboratory and started my project. Without his expertise in the field and patience to teach me who was the beginner in the field, I would not be able to finish this study.

I would like to thank Prof. Hajime Watanabe and Prof. Susumu Uchiyama who have taken their time to read and gave valuable comments on this dissertation.

I would like to acknowledge Dr. Matthew Daniels (Oxford University) who has given valuable comments on my experiment and proofread my manuscript.

Thanks are given to all Nagai Laboratory members for all the support through my stay in Nagai Laboratory especially Ms. Kazuyo Sakai, Ms. Aya Hisatomi, Dr. Shigenori Inagaki, Mr. Hajime Shinoda, Mr. Tran Quang and Ms. Israt Farhana.

I would like to acknowledge Indonesian Government for the financial support throguh the Indonesia Endowment Fund for Education during my study in Japan.

Last but not least, I would like to thank my family and friends for their constant encouragement that keeps me moving forward.

REFERENCES

Adams, S.R., Campbell, R.E., Gross, L.A., Martin, B.R., Walkup, G.K., Yao, Y., Llopis, J., and Tsien, R.Y. (2002). New biarsenical ligands and tetracysteine motifs for protein labeling in vitro and in vivo: Synthesis and biological applications. J. Am. Chem. Soc. *124*, 6063–6076.

Baptista, M.S., Cadet, J., Di Mascio, P., Ghogare, A.A., Greer, A., Hamblin, M.R., Lorente, C., Nunez, S.C., Ribeiro, M.S., Thomas, A.H., et al. (2017). Type I and Type II Photosensitized Oxidation Reactions: Guidelines and Mechanistic Pathways. Photochem. Photobiol. *93*, 912–919.

Barnett, M.E., Baran, T.M., Foster, T.H., and Wojtovich, A.P. (2018). Quantification of light-induced miniSOG superoxide production using the selective marker, 2-hydroxyethidium. Free Radic. Biol. Med. *116*, 134–140.

Baumgart, F., Rossi, A., and Verkman, A.S. (2012). Light inactivation of water transport and protein–protein interactions of aquaporin–Killer Red chimeras. J. Gen. Physiol. *139*, 83–91.

Bäumler, W., Regensburger, J., Knak, A., Felgenträger, A., and Maisch, T. (2012). UVA and endogenous photosensitizers – the detection of singlet oxygen by its luminescence. Photochem. Photobiol. Sci. *11*, 107–117.

Beermann, A.E.L., and Jay, D.G. (1994). Chapter 37 Chromophore-Assisted Laser Inactivation of Cellular Proteins. In Methods in Cell Biology, pp. 715–732.

Bresolí-Obach, R., Nos, J., Mora, M., Sagristà, M.L., Ruiz-González, R., and Nonell, S. (2016). Anthracene-based fluorescent nanoprobes for singlet oxygen detection in biological media. Methods *109*, 64–72.

Buckley, C., Carvalho, M.T., Young, L.K., Rider, S.A., McFadden, C., Berlage, C., Verdon, R.F., Taylor, J.M., Girkin, J.M., and Mullins, J.J. (2017). Precise spatio-temporal control of rapid optogenetic cell ablation with mem-KillerRed in Zebrafish. Sci. Rep. *7*, 5096.

Bulina, M.E., Chudakov, D.M., Britanova, O. V, Yanushevich, Y.G., Staroverov, D.B., Chepurnykh, T. V, Merzlyak, E.M., Shkrob, M.A., Lukyanov, S., and Lukyanov, K.A. (2006). A genetically encoded photosensitizer. Nat. Biotechnol. *24*, 95–99.

Campbell, R.E., Campbell, R.E., Tour, O., Tour, O., Palmer, A.E., Palmer, A.E., Steinbach, P. a, Steinbach, P. a, Baird, G.S., Baird, G.S., et al. (2002). A monomeric red fluorescent protein. Proc. Natl. Acad. Sci. U. S. A. *99*, 7877–7882.

Carpentier, P., Violot, S., Blanchoin, L., and Bourgeois, D. (2009). Structural basis for the phototoxicity of the fluorescent protein KillerRed. FEBS Lett. *583*, 2839–2842.

Chu, K.F., and Dupuy, D.E. (2014). Thermal ablation of tumours: Biological mechanisms and advances in therapy. Nat. Rev. Cancer *14*, 199–208.

D'Autréaux, B., and Toledano, M.B. (2007). ROS as signalling molecules: Mechanisms that generate specificity in ROS homeostasis. Nat. Rev. Mol. Cell Biol. *8*, 813–824.

Deisseroth, K. (2011). Optogenetics. Nat. Methods *8*, 26–29.

Dormann, D., Libotte, T., Weijer, C.J., and Bretschneider, T. (2002). Simultaneous quantification of cell motility and protein-membrane-association using active contours. Cell Motil. Cytoskeleton *52*, 221–230.

Foote, C.S. (1991). Definition of Type I and Type II Photosensitized Oxidation.

Photochem. Photobiol. *54*, 659–659.
He, J., Wang, Y., Missinato, M.A., Onuoha, E., Perkins, L.A., Watkins, S.C., St Croix, C.M., Tsang, M., and Bruchez, M.P. (2016). A genetically targetable near-infrared photosensitizer. Nat. Methods *13*, 263–268.
Hearps, A.C., Pryor, M.J., Kuusisto, H. V., Rawlinson, S.M., Piller, S.C., and Jans, D.A. (2007). The biarsenical dye lumio™ exhibits a reduced ability to specifically detect tetracysteine-containing proteins within live cells. J. Fluoresc. *17*, 593–597.
Hell, S.W. (2003). Toward fluorescence nanoscopy. Nat. Biotechnol. *21*, 1347–1355.
Hell, S.W., and Wichmann, J. (1994). Breaking the diffraction resolution limit by stimulated emission: stimulated-emission-depletion fluorescence microscopy. Opt. Lett. *19*, 780.
Hoffman-Kim, D., Kerner, J.A., Chen, A., Xu, A., Wang, T.F., and Jay, D.G. (2002). pp60c-srcis a negative regulator of laminin-1-mediated neurite outgrowth in chick sensory neurons. Mol. Cell. Neurosci. *21*, 81–93.
Jacobson, K., Rajfur, Z., Vitriol, E., and Hahn, K. (2008). Chromophore-assisted laser inactivation in cell biology. Trends Cell Biol. *18*, 443–450.
Jarvela, T., and Linstedt, A.D. (2014). Isoform-specific tethering links the Golgi ribbon to maintain compartmentalization. Mol. Biol. Cell *25*, 133–144.
Jay, D.G. (1988). Selective destruction of protein function by chromophore-assisted laser inactivation. Proc. Natl. Acad. Sci. *85*, 5454–5458.
Jay, D.G., and Keshishian, H. (1990). Laser inactivation of fasciclin I disrupts axon adhesion of grasshopper pioneer neurons. Nature *348*, 548–550.
Jay, D.G., and Sakurai, T. (1999). Chromophore-assisted laser inactivation (CALI) to elucidate cellular mechanisms of cancer. Biochim. Biophys. Acta - Rev. Cancer *1424*.
Keppler, A., and Ellenberg, J. (2009). Chromophore-assisted laser inactivation of alpha- and gamma-tubulin SNAP-tag fusion proteins inside living cells. ACS Chem. Biol. *4*, 127–138.
Kiermayer, C., Conrad, M., Schneider, M., Schmidt, J., and Brielmeier, M. (2007). Optimization of spatiotemporal gene inactivation in mouse heart by oral application of tamoxifen citrate. Genesis *45*, 11–16.
Kim, D.H., and Rossi, J.J. (2008). RNAi mechanisms and applications. Biotechniques *44*, 613–616.
Kim, K., Lakhanpal, G., Lu, H.E., Khan, M., Suzuki, A., Kato-Hayashi, M., Narayanan, R., Luyben, T.T., Matsuda, T., Nagai, T., et al. (2015). A Temporary Gating of Actin Remodeling during Synaptic Plasticity Consists of the Interplay between the Kinase and Structural Functions of CaMKII. Neuron *87*, 813–826.
Kim, S., Tachikawa, T., Fujitsuka, M., and Majima, T. (2014). Far-red fluorescence probe for monitoring singlet oxygen during photodynamic therapy. J. Am. Chem. Soc. *136*, 11707–11715.
Kobayashi, J., Shidara, H., Morisawa, Y., Kawakami, M., Tanahashi, Y., Hotta, K., and Oka, K. (2013). A method for selective ablation of neurons in C. elegans using the phototoxic fluorescent protein, KillerRed. Neurosci. Lett. *548*, 261–264.
Laissue, P.P., Alghamdi, R.A., Tomancak, P., Reynaud, E.G., and Shroff, H. (2017). Assessing phototoxicity in live fluorescence imaging. Nat. Methods *14*, 657–661.
Lee, S., Park, H., Kyung, T., Kim, N.Y., Kim, S., Kim, J., and Heo, W. Do (2014). Reversible protein inactivation by optogenetic trapping in cells. Nat. Methods *11*, 633–636.

Liao, J.C., Roider, J., and Jay, D.G. (1994). Chromophore-assisted laser inactivation of proteins is mediated by the photogeneration of free radicals. Proc. Natl. Acad. Sci. *91*, 2659–2663.

Liao, J.C., Berg, L.J., and Jay, D.G. (1995). Chromophore-Assisted Laser Inactivation of Subunits of the T-Cell Receptor in Living Cells is Spatially Restricted. Photochem. Photobiol. *62*, 923–929.

Liao, Z.X., Li, Y.C., Lu, H.M., and Sung, H.W. (2014). A genetically-encoded KillerRed protein as an intrinsically generated photosensitizer for photodynamic therapy. Biomaterials *35*, 500–508.

Lindig, B.A., Rodgers, M.A.J., and Schaaplc, A.P. (1980). Determination of the Lifetime of Singlet Oxygen in D20 Using 9,10-Anthracenedipropionic Acid, a Water-Soluble Probe. J. Am. Chem. Soc. *102*, 5590–5593.

Makhijani, K., To, T.L., Ruiz-González, R., Lafaye, C., Royant, A., and Shu, X. (2017). Precision Optogenetic Tool for Selective Single- and Multiple-Cell Ablation in a Live Animal Model System. Cell Chem. Biol. *24*, 110–119.

Marek, K.W., and Davis, G.W. (2002). Transgenically encoded protein photoinactivation (FlAsH-FALI): Acute inactivation of synaptotagmin I. Neuron *36*, 805–813.

Martin, B.R., Giepmans, B.N.G., Adams, S.R., and Tsien, R.Y. (2005). Mammalian cell-based optimization of the biarsenical-binding tetracysteine motif for improved fluorescence and affinity. Nat. Biotechnol. *23*, 1308–1314.

McCaffrey, A.P., Meuse, L., Pham, T.-T.T., Conklin, D.S., Hannon, G.J., and Kay, M. a (2002). RNA interference in adult mice. Nature *418*, 38–39.

McLean, M.A., Rajfur, Z., Chen, Z., Humphrey, D., Yang, B., Sligar, S.G., and Jacobson, K. (2009). Mechanism of Chromophore Assisted Laser Inactivation Employing Fluorescent Proteins. Anal. Chem. *81*, 1755–1761.

Mironova, K.E., Proshkina, G.M., Ryabova, A. V., Stremovskiy, O.A., Lukyanov, S.A.G. encoded immunophotosensitizer 4D5scFv-miniSOG is a highly selective agent for targeted photokilling of tumor cells in vitro, Petrov, R. V., and Deyev, S.M. (2013). Genetically encoded immunophotosensitizer 4D5scFv-miniSOG is a highly selective agent for targeted photokilling of tumor cells in vitro. Theranostics *3*, 831–840.

Moyano, D.F., and Rotello, V.M. (2011). Nano meets biology: Structure and function at the nanoparticle interface. Langmuir *27*, 10376–10385.

Nagel, G., Szellas, T., Huhn, W., Kateriya, S., Adeishvili, N., Berthold, P., Ollig, D., Hegemann, P., and Bamberg, E. (2003). Channelrhodopsin-2, a directly light-gated cation-selective membrane channel. Proc. Natl. Acad. Sci. *100*, 13940–13945.

Natsume, T., and Kanemaki, M.T. (2017). Conditional Degrons for Controlling Protein Expression at the Protein Level. Annu. Rev. Genet. *51*, 83–102.

Pimenta, F.M., Jensen, R.L., Breitenbach, T., Etzerodt, M., and Ogilby, P.R. (2013). Oxygen-dependent photochemistry and photophysics of "miniSOG," a protein-encased flavin. Photochem. Photobiol. *89*, 1116–1126.

Pletnev, S., Gurskaya, N.G., Pletneva, N. V., Lukyanov, K.A., Chudakov, D.M., Martynov, V.I., Popov, V.O., Kovalchuk, M. V., Wlodawer, A., Dauter, Z., et al. (2009). Structural basis for phototoxicity of the genetically encoded photosensitizer KillerRed. J. Biol. Chem. *284*, 32028–32039.

Rajfur, Z., Roy, P., Otey, C., Romer, L., and Jacobson, K. (2002). Dissecting the link between stress fibres and focal adhesions by CALI with EGFP fusion proteins. Nat. Cell Biol. *4*, 286–293.

De Rosny, E., and Carpentier, P. (2012). GFP-like phototransformation mechanisms in the cytotoxic fluorescent protein killerred unraveled by structural and spectroscopic investigations. J. Am. Chem. Soc. *134*, 18015–18021.

Rost, B.R., Schneider-Warme, F., Schmitz, D., and Hegemann, P. (2017). Optogenetic Tools for Subcellular Applications in Neuroscience. Neuron *96*, 572–603.

Ruiz-González, R., Cortajarena, A.L., Mejias, S.H., Agut, M., Nonell, S., and Flors, C. (2013). Singlet oxygen generation by the genetically encoded tag minisog. J. Am. Chem. Soc. *135*, 9564–9567.

Ryumina, A.P., Serebrovskaya, E.O., Shirmanova, M. V., Snopova, L.B., Kuznetsova, M.M., Turchin, I. V., Ignatova, N.I., Klementieva, N. V., Fradkov, A.F., Shakhov, B.E., et al. (2013). Flavoprotein miniSOG as a genetically encoded photosensitizer for cancer cells. Biochim. Biophys. Acta - Gen. Subj. *1830*, 5059–5067.

Ryumina, A.P., Serebrovskaya, E.O., Staroverov, D.B., Zlobovskaya, O.A., Shcheglov, A.S., Lukyanov, S.A., and Lukyanov, K.A. (2016). Lysosome-associated minisog as a photosensitizer for Mammalian cells. Biotechniques *61*, 92–94.

Saito, K., Chang, Y.F., Horikawa, K., Hatsugai, N., Higuchi, Y., Hashida, M., Yoshida, Y., Matsuda, T., Arai, Y., and Nagai, T. (2012). Luminescent proteins for high-speed single-cell and whole-body imaging. Nat. Commun. *3*.

Saito, M., Iwawaki, T., Taya, C., Yonekawa, H., Noda, M., Inui, Y., Mekada, E., Kimata, Y., Tsuru, A., and Kohno, K. (2001). Diphtheria toxin receptor-mediated conditional and targeted cell ablation in transgenic mice. Nat. Biotechnol. *19*, 746–750.

Sarkisyan, K.S., Zlobovskaya, O.A., Gorbachev, D.A., Bozhanova, N.G., Sharonov, G. V., Staroverov, D.B., Egorov, E.S., Ryabova, A. V., Solntsev, K.M., Mishin, A.S., et al. (2015). KillerOrange, a genetically encoded photosensitizer activated by blue and green light. PLoS One *10*.

Schieber, M., and Chandel, N.S. (2014). ROS function in redox signaling and oxidative stress. Curr. Biol. *24*.

Schindler, S.E., McCall, J.G., Yan, P., Hyrc, K.L., Li, M., Tucker, C.L., Lee, J.M., Bruchas, M.R., and Diamond, M.I. (2015). Photo-activatable Cre recombinase regulates gene expression in vivo. Sci. Rep. *5*.

Schneider, C., Rasband, W., and Eliceiri, K. (2012). ImageJ. Nat. Methods *9*, 671–675.

Schwartzberg, P.L., Goff, S.P., and Robertson, E.J. (1989). Germ-line transmission of a c-abl mutation produced by targeted gene disruption in ES cells. Science *246*, 799–803.

Serebrovskaya, E.O., Edelweiss, E.F., Stremovskiy, O.A., Lukyanov, K.A., Chudakov, D.M., and Deyev, S.M. (2009). Targeting cancer cells by using an antireceptor antibody-photosensitizer fusion protein. Proc. Natl. Acad. Sci. U. S. A. *106*, 9221–9225.

Serebrovskaya, E.O., Ryumina, A.P., Boulina, M.E., Shirmanova, M. V., Zagaynova, E. V., Bogdanova, E.A., Lukyanov, S.A., and Lukyanov, K.A. (2013). Phototoxic effects of lysosome-associated genetically encoded photosensitizer KillerRed. J. Biomed. Opt. *19*, 071403.

Shah, E.M., and Jay, D.G. (1993). Methods for ablating neurons. Curr. Opin. Neurobiol. *3*, 738–742.

Shaner, N.C., Campbell, R.E., Steinbach, P.A., Giepmans, B.N.G., Palmer, A.E., and

Tsien, R.Y. (2004). Improved monomeric red, orange and yellow fluorescent proteins derived from Discosoma sp. red fluorescent protein. Nat. Biotechnol. *22*, 1567–1572.

Shirmanova, M., Yuzhakova, D., Snopova, L., Perelman, G., Serebrovskaya, E., Lukyanov, K., Turchin, I., Subochev, P., Lukyanov, S., Kamensky, V., et al. (2015). Towards PDT with genetically encoded photosensitizer killerred: A comparison of continuous and pulsed laser regimens in an animal tumor model. PLoS One *10*.

Shirmanova, M. V., Serebrovskaya, E.O., Lukyanov, K.A., Snopova, L.B., Sirotkina, M.A., Prodanetz, N.N., Bugrova, M.L., Minakova, E.A., Turchin, I. V., Kamensky, V.A., et al. (2013a). Phototoxic effects of fluorescent protein KillerRed on tumor cells in mice. J. Biophotonics *6*, 283–290.

Shirmanova, M. V, Serebrovskaya, E.O., Snopova, L.B., Kuznetsova, M.M., Ryumina, A.P., Turchin, I. V, Sergeeva, E.A., Ignatova, N.I., Klementieva, N. V, and Lukyanov, K.A. (2013b). KillerRed and miniSOG as genetically encoded photosensitizers for photodynamic therapy of cancer. Eur. Conf. Biomed. Opt. *8803*, 88030L–88030L.

Shu, X., Lev-Ram, V., Deerinck, T.J., Qi, Y., Ramko, E.B., Davidson, M.W., Jin, Y., Ellisman, M.H., and Tsien, R.Y. (2011). A genetically encoded tag for correlated light and electron microscopy of intact cells, tissues, and organisms. PLoS Biol. *9*.

Stroffekova, K., Proenza, C., and Beam, K.G. (2001). The protein-labeling reagent FLASH-EDT2 binds not only to CCXXCC motifs but also non-specifically to endogenous cysteine-rich proteins. Pflugers Arch. Eur. J. Physiol. *442*, 859–866.

Surrey, T., Elowitz, M.B., Wolf, P.E., Yang, F., Nédélec, F., Shokat, K., and Leibler, S. (1998). Chromophore-assisted light inactivation and self-organization of microtubules and motors. Proc. Natl. Acad. Sci. U. S. A. *95*, 4293–4298.

Suzuki, K., Kimura, T., Shinoda, H., Bai, G., Daniels, M.J., Arai, Y., Nakano, M., and Nagai, T. (2016). Five colour variants of bright luminescent protein for real-time multicolour bioimaging. Nat. Commun. *7*.

Takemoto, K., Matsuda, T., McDougall, M., Klaubert, D.H., Hasegawa, A., Los, G. V., Wood, K. V., Miyawaki, A., and Nagai, T. (2011). Chromophore-assisted light inactivation of HaloTag fusion proteins labeled with eosin in living cells. In ACS Chemical Biology, pp. 401–406.

Takemoto, K., Matsuda, T., Sakai, N., Fu, D., Noda, M., Uchiyama, S., Kotera, I., Arai, Y., Horiuchi, M., Fukui, K., et al. (2013a). SuperNova, a monomeric photosensitizing fluorescent protein for chromophore-assisted light inactivation. Sci. Rep. *3*, 2629.

Takemoto, K., Matsuda, T., Sakai, N., Fu, D., Noda, M., Uchiyama, S., Kotera, I., Arai, Y., Horiuchi, M., Fukui, K., et al. (2013b). SuperNova, a monomeric photosensitizing fluorescent protein for chromophore-assisted light inactivation. Sci. Rep. *3*.

Takemoto, K., Iwanari, H., Tada, H., Suyama, K., Sano, A., Nagai, T., Hamakubo, T., and Takahashi, T. (2016). Optical inactivation of synaptic AMPA receptors erases fear memory. Nat. Biotechnol. *35*, 38–47.

Teh, C., and Korzh, V. (2014). In vivo optogenetics for light-induced oxidative stress in transgenic zebrafish expressing the KillerRed photosensitizer protein. Methods Mol. Biol. *1148*, 229–238.

Thomas, K.R., and Capecchi, M.R. (1987). Site-directed mutagenesis by gene targeting in mouse embryo-derived stem cells. Cell *51*, 503–512.

Tubbs, J.L., Tainer, J.A., and Getzoff, E.D. (2005). Crystallographic structures of Discosoma red fluorescent protein with immature and mature chromophores: Linking peptide bond trans-cis isomerization and acylimine formation in chromophore maturation. Biochemistry *44*, 9833–9840.

Valon, L., Marín-Llauradó, A., Wyatt, T., Charras, G., and Trepat, X. (2017). Optogenetic control of cellular forces and mechanotransduction. Nat. Commun. *8*.

Várnai, P., and Balla, T. (1998). Visualization of phosphoinositides that bind pleckstrin homology domains: calcium-and agonist-induced dynamic changes and relationship to myo- inositol-. J. Cell Biol. *143*, 501–510.

Varshavsky, A. (1991). Naming a targeting signal. Cell *64*, 13–15.

Vegh, R.B., Solntsev, K.M., Kuimova, M.K., Cho, S., Liang, Y., Loo, B.L.W., Tolbert, L.M., and Bommarius, A.S. (2011). Reactive oxygen species in photochemistry of the red fluorescent protein "Killer Red." Chem. Commun. *47*, 4887.

Vitriol, E.A., Wise, A.L., Berginski, M.E., Bamburg, J.R., and Zheng, J.Q. (2013). Instantaneous inactivation of cofilin reveals its function of F-actin disassembly in lamellipodia. Mol. Biol. Cell *24*, 2238–2247.

Wang, F.-S., and Jay, D.G. (1996). Chromophore-assisted laser inactivation (CALI): probing protein functionin situ with a high degree of spatial and temporal resolution. Trends Cell Biol. *6*, 442–445.

Westberg, M., Holmegaard, L., Pimenta, F.M., Etzerodt, M., and Ogilby, P.R. (2015). Rational design of an efficient, genetically encodable, protein-encased singlet oxygen photosensitizer. J. Am. Chem. Soc. *137*, 1632–1642.

Westberg, M., Bregnhøj, M., Etzerodt, M., and Ogilby, P.R. (2017). No Photon Wasted: An Efficient and Selective Singlet Oxygen Photosensitizing Protein. J. Phys. Chem. B *121*, 9366–9371.

Williams, D.C., ElBejjani, R., Ramirez, P., Coakley, S., Kim, S.A., Lee, H., Wen, Q., Samuel, A., Lu, H., Hilliard, M.A., et al. (2013). Rapid and Permanent Neuronal Inactivation InVivo via Subcellular Generation of Reactive Oxygen with the Use of KillerRed. Cell Rep. *5*, 553–563.

Winterbourn, C.C. (2008). Reconciling the chemistry and biology of reactive oxygen species. Nat Chem Biol *4*, 278–286.

Wu, Y.H., Franden, M.A., Hawker, J.R., McHenry, C.S., Silver, P., Losick, R., Grossman, A., Wright, A., and Losick, R. (1984). Monoclonal antibodies specific for the alpha subunit of the Escherichia coli DNA polymerase III holoenzyme. J. Biol. Chem. *259*, 12117–12122.

Zorov, D.B., Filburn, C.R., Klotz, L.O., Zweier, J.L., and Sollott, S.J. (2000). Reactive oxygen species (ROS)-induced ROS release: A new phenomenon accompanying induction of the mitochondrial permeability transition in cardiac myocytes. J Exp Med *192*, 1001–1014.

ACHIEVEMENTS

Peer reviewed journal article

Riani YD, Matsuda T, Nagai T. Green monomeric photosensitizing fluorescent protein for photo-inducible protein inactivation and cell ablation. *BMC Biol*. 2018; 16: 50.

Book chapter

Nagai T, **Riani YD**. Optogenetic control of reactive oxygen species generation for photo-inducible protein inactivation and cell ablation. In: Vriz, S, Ozawa, T, editors. Optogenetics. Cambridge: Royal Society of Chemistry Books. **In Press** March 2018.

Oral presentations

Toward multi-spatiotemporal control of protein inactivation and cell ablation. Janelia Junior Scientist Workshop on Protein Engineering, Howard Hughes Medical Institute, Janelia Research Campus, Ashburn, VA. March 6, 2018.

Poster presentations

Development of SuperNova Green for selective cell ablation. QBiC Symposium 2016: Decoding Organisms by Quantitative Cell Profiling. Osaka, Japan. September, 2016

Green variant of monomeric photosensitizing fluorescent protein for photo-inducible protein inactivation and cell ablation. Kageyama Scientific Research on Innovative Areas. Shizuoka, Japan, January 2017

Development of monomeric green variant genetically encoded photosensitizer for photo-inducible protein inactivation and cell ablation. Single-Cell Biophysics: Measurement, Modulation, and Modeling. Taipei, Taiwan. June, 2017

SUPPLEMENTARY DATA

Table S1. List of oligonucleotides used in this study

Y66W Forward primer	5'-TGG GGC GAG CCC TTC TTC-3'
Y66W Reverse primer	5'-CTG GAT CAG GTG GCA GAT GGG-3'
V44A Forward primer	5'-GCG CAC GCC GTG TGC GAG-3'
V44A Reverse primer	5'-GCG CAC GCC GTG TGC GAG-3'
BamHI-SuperNova Forward primer	5' - T TAG GAT CCG ATG GGT TCA GAG GTC GGC-3'
BamHI-SuperNova Forward primer (2)	5'-GC GGA TCC ATG GGT TCA GAG GTC GGC CCC-3'
EcoRI-stop codon-SuperNova Reverse primer	5'-GC GAA TTC TTA ATC CTC GTC GCT ACC GAT-3'
BamHI-miniSOG Forward primer	5'-A ATG GAT CCG ATG GGA AAA GAG CTT TG-3'
EcoRI-stop codon-miniSOG Reverse primer	5'-AAT GAA TTC TTA TCC ATC CAG CTG CAC-3'
HindIII-SuperNova Forward primer	5'-TA AAG CTT ATGG GTT CAG AGG TCG GC-3'
BamHI-stop codon-SuperNovaΔ11 Reverse primer	5'-TA GGA TCC GGG CAC GCT GTG G-3'
EcoRI-SuperNova Reverse primer	5'-GTA GAA TTC TTG ATC CTC GTC GCT ACC GAT GGC-3'
AgeI-kozak-Venus Forward primer	5'-T ATA CCG GTC CGC ACC ATG GTG AGC AAG GGC GAG-3'
BglII-linker-Venus Reverse primer	5'-TA AGA TCT GAG TCC GGA CTT GTA CAG CTC GTC CAT GCC GAG-3'
XbaI-SuperNova Forward primer	5'-AAG TCT AGA ATG GGT TCA GAG GTC GGC C-3'
AgeI-kozak sequence-mNeptune Forward primer	5'-A TAC CGG TCC ACC ATG GTG TCT AAG GGC GAA-3'
BglII-mNeptune Reverse primer	5'-GC TCT AGA TTA ATC CTC GTC GCT ACC G-3'

Supplementary Data 1

Several attempts have been done to introduce site directed mutagenesis to SNR or mKillerOrange to produce green variants other than SNG. Below is listed important amino acid to in KillerRed and SNR based on their crystal structure analysis (Carpentier et al., 2009; Pletnev et al., 2009; Takemoto et al., 2013b).

Function	Residues	References
Monomerization	L160[1,2], F162[1,2], G3[1,2], N145[1,2], L172[1], M204[1]	[1] Takemoto et al., 2012 [2] Sarkisyan et al., 2015 [3] Pletnev et al., 2009 [4] Carpentier et al., 2009 [5] Pletneva et al., 2015 [6] Rosny et al., 2012
Water channel and ROS generation	I142[3], L143[3], P144[3], I199[3], I200[3], T201[3], P69[3], I199[3], R94[3], E218[3], F81[4], M149[4], V157[4], M181[4], P192[4], P154[4], E190[4], I199[4,5], E68[4], S119[4], M204[4], C215[4], A161[4]	
Chromophore and surroundings	E68[3,4], S119[3], N145[1,2,3], T201[3,4,5], Q159[3,5], F14[3],F42[3], F70[3], F71[3], Y110[3], I16[3], Q65[4], V44[4], E218[6], I163[6], F177[2,6], G218[5], R94[5], D113[2], Y221[2], E236[2]	

Based on those collected studies above, random site directed mutagenesis were introduced into mKillerOrange-pRSET$_B$ with QuikChange or inverse PCR method. List of oligonucleotides used for this experiment is listed below:

E68N Forward primer	5’- NNS CCC TTC TTC GCC CGC TAC -3’
E68N Reverse primer	5' - GCC GTA CTG GAT CAG GTG -3'
T201N Forward primer	5'- NNS AAG CAG ACG AGG GAC ACT -3'
T201N Reverse primer	5'- GAT GAT GGT CAC GAA GTG -3'
KillerRed Q65T Quikchange primer	5’- GC CAC CTG ATC ACC TAC GGC GAG -3’
SNR E68N Quikchange primer	5’- G ATC CAG TAC GGC NNN CCC TTC TTC -3’
mKillerOrange E68N Quikchange primer	5’- G ATC CAG TGG GGC NNN CCC TTC TTC -3’

Plasmids were transformed into *E.coli* JM109(DE3) then colonies were picked and spreaded onto cover glass. Emission spectra of the protein expressed on the colonies were taken with confocal microscope (FV1000, Olympus) equipped with 488 nm excitation light (multi-Argon ion laser). Below is shown the emission spectrum of several mutated SNG and mKillerOrange.

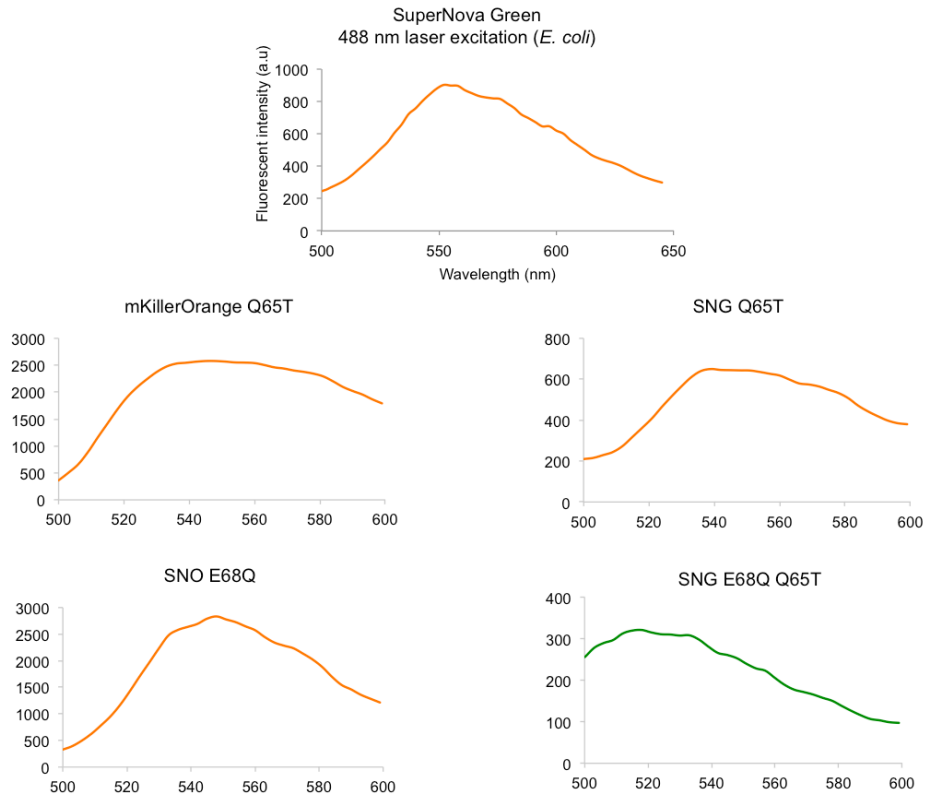

Figure S1. Emission spectrum of SNG and several mutated versions of SNG and mKillerOrange in *E. coli* cells taken with 488 nm laser excitation light.

Due to the presence of maturated orange chromophore in SNG, excitation with 488 nm light results in ~550 nm emission peak. Noted several additional mutation into SNG resulted in blue-shifted emission peak, presumably indicates fully immatured form of intermediate green chromophore. Other trials on site directed mutagenesis did not show any emission changes during screening process (data not shown).